



Metabolite Profiling of Antioxidant Rich Fractions of *Punica granatum* L. Mesocarp and CD36 Expression Regulation

Piteesha Ramlagan, Marwa Yousry Issa, Philippe Rondeau, Emmanuel Bourdon, Theeshan Bahorun, Mohamed A. Farag & Vidushi S Neergheen

To cite this article: Piteesha Ramlagan, Marwa Yousry Issa, Philippe Rondeau, Emmanuel Bourdon, Theeshan Bahorun, Mohamed A. Farag & Vidushi S Neergheen (2023) Metabolite Profiling of Antioxidant Rich Fractions of *Punica granatum* L. Mesocarp and CD36 Expression Regulation, Journal of the American Nutrition Association, 42:1, 36-54, DOI: 10.1080/07315724.2021.1978349

To link to this article: <https://doi.org/10.1080/07315724.2021.1978349>



Published online: 22 Oct 2021.



Submit your article to this journal [↗](#)



Article views: 119




View related articles [↗](#)



View Crossmark data [↗](#)



Metabolite Profiling of Antioxidant Rich Fractions of *Punica granatum* L. Mesocarp and CD36 Expression Regulation

Piteesha Ramlagan^{a,b}, Marwa Yousry Issa^c, Philippe Rondeau^d, Emmanuel Bourdon^d,
Theeshan Bahorun^{a,e,f}, Mohamed A. Farag^{c,g}  and Vidushi S. Neerghen^a

^aBiopharmaceutical Unit, Centre for Biomedical and Biomaterials Research, MSIRI Building, University of Mauritius, Réduit, Mauritius; ^bDepartment of Health Sciences, Faculty of Medicine and Health Sciences, University of Mauritius, Réduit, Mauritius; ^cPharmacognosy Department, College of Pharmacy, Cairo University, Cairo, Egypt; ^dUniversité de La Réunion, INSERM, UMR 1188 Diabète athérothrombose Thérapies Réunion Océan Indien (DÉTRO), Saint-Denis de La Réunion, France; ^eDepartment of Biosciences and Ocean Studies, Faculty of Science, University of Mauritius, Réduit, Mauritius; ^fMauritius Research Innovation Council, Ebène, Mauritius; ^gChemistry Department, School of Sciences & Engineering, The American University in Cairo, New Cairo, Egypt

ABSTRACT

Objective: It was aimed at determining which polyphenolic compound(s) in pomegranate mesocarp extract (PME) is liable for the antioxidant, anti-glycation and anti-CD36 activities.

Methods: The PME was fractionated using liquid-liquid extraction method. The fractions were tested for their polyphenolic content, antioxidant potency, anti-glycation activity and anti-CD36 potential. The metabolite compositions of PME and derived fractions were investigated in an untargeted manner using metabolomics in relation to its antioxidant and anti-glycation activities.

Results: The ethyl acetate and *n*-butanol fractions of the pomegranate mesocarp demonstrated highest antioxidant and anti-glycation potencies. These fractions, represented by gallic and ellagic acids monomers, were enriched in tannins and phenolic acids. Orthogonal partial least squares discriminant analysis (OPLS-DA) modeling of ultra-performance liquid chromatography-mass spectrometry (UPLC-MS) metabolite profiles from the different pomegranate mesocarp fractions indicated that gallic and ellagic acids were potential contributors to the antioxidant and anti-glycation effects of the pomegranate mesocarp. At cellular level, the polyphenolic-rich crude extract as well as the ethyl acetate, *n*-butanol and aqueous residual fractions suppressed the protein expression of CD36. The anti-CD36 activity of these extracts and fractions was attributed to the presence of punicalagin, the ellagitannins that occurred in equal amount in the different fractions.

Conclusion: This work demonstrated the protective effect of the non-edible part of the pomegranate fruit and showed that gallic and ellagic acids account for the antioxidant and anti-glycation activities while punicalagin is liable for the anti-CD36 activity of PME.

ARTICLE HISTORY

Received 5 August 2021
Accepted 2 September 2021

KEYWORDS




Pomegranate mesocarp extract; fractionation; OPLS-DA modeling; anti-diabetic potency; punicalagin


Introduction

Type 2 diabetes mellitus (T2DM) is a metabolic disorder that affects at least 463 million people worldwide and is predicted to increase to 700 million by 2045 (1,2). This chronic disease occurs as a consequence of insufficient insulin secretion and/or insulin resistance, which result in hyperglycemia. Sustained hyperglycemia contributes to the pathogenesis of diabetic complications such as neuropathy, nephropathy, retinopathy and cardiovascular disease (3). The excess of sugar that occurs in the hyperglycemic condition induces the glycation of proteins to form Schiff bases and Amadori products, which rearrange to dicarbonyls such as methylglyoxal (MGO) (4). Dicarbonyls eventually lead to the formation of harmful fluorescent and non-fluorescent advanced glycation end products (AGEs) (5). These glycated proteins bind to their corresponding receptors and induce an oxidative stress state by promoting an over-production

of reactive oxygen species (ROS) and by decreasing the activity of the intrinsic antioxidant defence system (6). This condition in turn promotes the secretion of pro-inflammatory mediators, which culminates to the development of diabetic complications (7).

CD36 is a known AGEs receptor that is over-expressed in different cell types (8). The deleterious effects of AGEs-CD36 binding has been widely reported as the interaction potentially induce inflammation, apoptosis of proximal tubular epithelial cell, liver fibrosis, platelet aggregation and occlusive thrombus formation (9–14). Being a multi-ligand receptor, CD36 is implicated in insulin resistance, atherosclerosis and dyslipidemia, due to its high binding affinity to additional ligands such as oxidized low-density lipoproteins, lipids and fatty acids (15). As such, binding of fatty acid metabolites to CD36 affects insulin-induced GLUT-4 translocation leading to decreased rate of glucose uptake and thus, hyperglycemia (16).

CONTACT Mohamed A. Farag  mohamed.alifarag@aucegypt.edu  Pharmacognosy Department, College of Pharmacy, Cairo University, Kasr el Aini St., P.B. 11562, Cairo, Egypt; Vidushi S. Neerghen  v.neerghen@uom.ac.mu Biopharmaceutical Unit, Centre for Biomedical and Biomaterials Research, MSIRI Building, University of Mauritius, Réduit, Republic of Mauritius.

 Supplemental data for this article is available online at <https://doi.org/10.1080/07315724.2021.1978349>.

Anti-CD36 compounds have been shown to decrease atherosclerotic lesions, to reduce postprandial hyperlipidemia and to increase insulin sensitivity (15). Moreover, insulin was shown to down-regulate the AGEs-induced CD36 over-expression in non-diabetic model. However, in diabetic model, suppression of CD36 by insulin did not occur, potentially due to impairment in the insulin signaling pathway (17). This thus provides scope for novel research aiming at identifying naturally occurring compounds with anti-CD36 activity in diabetics. We previously demonstrated that the pomegranate mesocarp extract (PME), which is a polyphenolic antioxidant-rich functional food, has the ability to down-regulate the expression of CD36 in the presence as well as the absence of AGEs. PME also demonstrated antioxidant effect by down-regulating AGEs-induced ROS level in addition to basal ROS level. Moreover, in a multi-assay antioxidant system, PME was shown to exert high antioxidant activity (18). PME is rich in hydrolyzable tannins, mainly ellagitannins, such as castalagin, casuarinin, granatin B, lagerstannin C, pedunculagin I, pedunculagin II, punicalagin, punigluconin and ellagic acid derivatives (19). Punicalagin, which is the predominant compound in PME, has been reported to exert the highest antioxidant activity among different pomegranate polyphenols (19,20). It is thus of interest to determine whether punicalagin accounts for the antioxidant and anti-CD36 activities as well as the anti-glycation potency in PME.

The main objective of this study was to explore the metabolite compositions of pomegranate mesocarp extract and derived fractions in an untargeted manner using metabolomics and in relation to its antioxidant and anti-glycation activity, as well as to assess the anti-CD36 activities of the mesocarp fractions.

Materials and methods

Chemicals

3T3-L1 cell line was obtained from American Type Tissue Culture (ATCC). Dulbecco's modified Eagle's medium (DMEM), fetal bovine serum (FBS) and 3,3',5,5'-tetramethylbenzidine (TMB) were from Thermo Fisher Scientific. All other chemicals were obtained from Sigma-Aldrich unless otherwise stated.

Preparation of pomegranate mesocarp fractions

The ripe fruits of *Punica granatum* L. (voucher number: MAU 0016480) were obtained from a domesticated plant in 'Mahebourg' village, situated in the south-eastern part of Mauritius. The mesocarp was cleaned, freeze-dried and ground into a fine powder prior to extraction. The lyophilized mesocarp was exhaustively extracted by 70% methanol (1:3, w/v) at 4°C for 3 consecutive days. The filtrates were centrifuged and the supernatants were pooled together prior to concentration under reduced pressure followed by lyophilization. A total of 100 g of lyophilized mesocarp

extract was dissolved in distilled water and sequentially extracted with dichloromethane (DCM), ethyl acetate (EtAc) and *n*-butanol (BUT). The organic fractions were dried using sodium sulfate salt. The fractions, including the residual aqueous (Aq) fraction were filtered, evaporated under reduced pressure and lyophilized to obtain 0.282 g of DCM, 0.835 g of EtAc, 8.782 g of BUT and 89.421 g of Aq fractions. The crude extract and fractions were dissolved in dimethyl sulfoxide (DMSO) for subsequent assays.

Antioxidant activity of pomegranate mesocarp crude extract and fractions

The antioxidant capacities of the mesocarp crude extract and fractions were assessed using a multi antioxidant assay system. The control contained the extract vehicle instead of the sample and punicalagin was used as positive control. The chelating/scavenging activity of the sample in the different assays was calculated according to Equation (1) and results were expressed as mean AA₅₀ (µg LP/mL).

$$\text{Scavenging / chelating / inhibitory activity (\%)} = ((A_0 - A_1) / A_0) \times 100 \quad (1)$$

Where A₀ is absorbance of reaction mixture only and A₁ is absorbance of reaction mixture with the sample.

Ferric reducing antioxidant power (FRAP) assay

The ability of the mesocarp crude extract and fractions to reduce ferrous ions was assayed using the method adapted from Benzie et al. (21). The FRAP reagent was freshly prepared by mixing 20 mL of 10 mM 2,4,6-tri(2-pyridyl)-s-triazine (TPTZ) in 40 mM HCl and 20 mL of 20 mM ferric chloride in 200 mL of 0.25 M sodium acetate buffer (pH 3.6) followed by warming at 37°C. The final reaction mixture comprised 150 µL of distilled water, 1.5 mL of FRAP reagent and 50 µL of sample. The absorbance was read at 593 nm against a blank. Ferric reducing ability was calculated with respect to ferrous sulfate standard curve and results expressed in mmol Fe²⁺/g LP.

Oxygen radical absorbance capacity (ORAC) assay

The protective capacity of the mesocarp crude extract and fractions in suppressing 2,2'-azobis(2-methylpropionamide) dihydrochloride (AAPH)- induced decay in fluorescence of fluorescein was evaluated by the method adapted from Huang et al. (22) with modifications. The reaction was carried out in phosphate buffer (75 mM, pH 7.4). Briefly, 25 µL of each sample was incubated with 150 µL of 83 nM of fluorescein sodium at 37°C for 20 min in a 96-well black microplate. The fluorescence kinetic was measured at excitation and emission wavelengths of 485 and 530 nm, respectively for 2 h 15 min at 37°C immediately after addition of 25 µL of 153 mM AAPH. The results were based on the area under the curve (AUC) of fluorescence decay over time and compared with a calibration curve of Trolox. Results were expressed in mmol Trolox/g LP.

2,2'-Azino-bis(3-ethylbenzothiazoline-6-sulphonic acid) (ABTS) radical scavenging assay

The method described by Re et al. (23) with modification in the volumes was used. ABTS radicals (ABTS^{•+}) was prepared by dissolving ABTS in 2.45 mM potassium persulphate to a final concentration of 7 mM and allowing the reaction mixture to stand in dark at room temperature for 16 h. ABTS^{•+} formed was then diluted to an absorbance of 0.700 (\pm 0.02) at 734 nm, after which 50 μ L of different concentrations of the samples was incubated with 1.5 mL of the diluted ABTS^{•+} solution for 6 min at 30 °C. Absorbance was then measured at 734 nm. The scavenging activity of ABTS^{•+} was calculated according to Equation (1) and results were expressed as mean AA₅₀ (μ g LP/mL).

2,2-Diphenyl-1-picrylhydrazyl (DPPH) radical scavenging assay

The method described by Duan et al. (24) was used. Briefly, 0.1 mL of different concentrations of the samples was incubated with 2.9 mL of 0.1 mM methanolic DPPH radicals (DPPH[•]) at 25 °C for 30 min in the dark. The absorbance was measured at 517 nm. Scavenging activity of DPPH[•] was calculated according to Equation (1) and results were expressed as mean AA₅₀ (μ g LP/mL).

Iron (II) (Fe²⁺) chelating assay

The chelating potential was assayed as described by Dorman et al. (25). Briefly, 200 μ L of different concentrations of the samples was mixed with 50 μ L of 0.5 mM iron (II) chloride. Following addition of 750 μ L distilled deionized water, the reaction mixture was incubated for 5 min at room temperature, after which 50 μ L of 2.5 mM ferrozine was added. The absorbance was measured at 562 nm before and after the addition of ferrozine. The chelating activity was calculated according to Equation (1) and results were expressed as mean AA₅₀ (μ g LP/mL).

Superoxide radical (O₂⁻) scavenging assay

O₂⁻ scavenging by the mesocarp crude extract and fractions was determined as described by Kumar et al. (26) with some modifications in volume and concentration. A total of 0.25 mL of different concentrations of the samples was mixed with 1 mL of 156 μ M nitroblue tetrazolium (NBT) solution and 1 mL of 200 μ M reduced β -nicotinamide adenine dinucleotide (NAD). The reaction was initiated following addition of 0.3 mL of 60 μ M phenazine methosulphate solution (PMS). The absorbance was measured at 560 nm after incubation at 25 °C for 30 min. The scavenging activity was calculated according to Equation (1) and results were expressed as mean AA₅₀ (μ g LP/mL).

Anti-glycation activity of pomegranate mesocarp crude extract and fractions

Bovine serum albumin (BSA) glycation using different glycation agents was performed according to Sompong et al.

(5) and Wang et al. (27) with modifications. Under sterile conditions, 10 mg/mL of BSA was incubated at 37 °C for 15 days with glucose (500 mM), ribose (100 mM) or MGO (25 mM) in phosphate buffer saline (PBS) (pH 7.4) in the presence or absence of 0.1 and 1 mg/ml of mesocarp crude extract and fractions. The reaction mixture was then used for assessment of levels of fluorescent AGEs, fructosamine, protein carbonyl content and AOPP.

Determination of AGEs formation

Formation of AGEs was spectrofluorometrically measured at an excitation and emission of 360 and 460 nm, respectively. The level of fluorescent AGEs produced was expressed as a percentage of unglycated BSA (28).

Determination of amadori products

Level of Amadori products was determined by incubating 10 μ L of reaction mixture with 100 μ L 0.5 mM NBT (in 100 mM carbonate buffer, pH 10.4) at 37 °C. Absorbance was measured at 530 nm after 10 min and 15 min. Results were expressed in mM of 1-deoxy-1-morpholino-D-fructose (1-DMF) (29).

Quantification of protein carbonyl

Accumulation of protein carbonyl was quantified using the enzyme-linked immunosorbent assay (ELISA) method (30). Briefly, 96-well ELISA plate (NUNC Maxisorp) was coated with 100 μ L of 10 μ g/mL protein sample and incubated overnight at 4 °C. After 45 min incubation with a solution of 0.04 mg/mL of 2,4-dinitrophenylhydrazine (DNP), the proteins were probed with an anti-DNP antibody for 1 h, followed by horseradish peroxidase conjugated secondary antibody for another 1 h. TMB substrate was then added and allowed to oxidize for 10 min. The reaction was stopped by the addition of 2 N hydrochloric acid, and absorbance was measured at 450 nm and 570 nm. Results are expressed as a percentage of vehicle treatment only.

Quantification of advanced oxidation protein products (AOPP)

AOPP level was quantified by addition of 10 μ L of acetic acid to 100 μ L sample. The optical density was measured at 340 nm and concentration of AOPP was calculated with respect to chloramine-T in presence of 1.16 M potassium iodide standard curve. Results were expressed in μ M chloramine-T equivalent per total protein concentration (31).

Cell culture of 3T3-L1

The mouse embryo 3T3-L1 preadipocyte was cultured in DMEM containing 25 mM glucose, 10% FBS, 2 mM L-glutamine, 100 μ g/mL streptomycin, 100 U/mL penicillin and 0.5 μ g/mL amphotericin B. The cell culture condition was in a humidified 5% CO₂ incubator at 37 °C.

Dimethylthiazol diphenyl tetrazolium (MTT) assay

A concentration of 10 µg/mL of mesocarp crude extract was previously demonstrated as the highest nontoxic concentration to the preadipocytes following 24 h treatment¹⁸. In this line, the potential cytotoxic effect of the 10 µg/mL of mesocarp fractions on preadipocytes was evaluated by the MTT and the lactate dehydrogenase release assays. Briefly, cells were plated overnight in 96-well plate at 1×10^4 cells/well. The cells were then treated with 10 µg/mL of mesocarp crude extract and fractions as well as punicalagin for 24 h. Following the treatment time, 200 µL of 0.5 mg/mL MTT solution was added to each well. After 3 h of incubation, 100 µL of DMSO was added and the absorbance was read at 590 nm and 690 nm. Results were expressed as percentage of control cells treated with vehicle only (32).

Lactate dehydrogenase assay

Lactate dehydrogenase (LDH) leakage from cells treated with 10 µg/mL of mesocarp crude extract/fractions and punicalagin was assessed by mixing 50 µL of supernatant, 50 µL 183 µM Tris (pH 8), 50 µL 204 mM lithium lactate and 50 µL of a mixture of 65 mM of INT (dissolved in DMSO), 29 mM of PMS and 5.5 mM NAD in a ratio of 1:1:23. The mixture was incubated for 10 min in dark and the absorbance was read at 490 nm. Cytotoxicity results were expressed as percentage of control.

Measurement of intracellular ROS production

The intracellular ROS level in preadipocytes was evaluated following 24 h treatment with 10 µg/mL of mesocarp crude extract/fractions and punicalagin. Following treatment in 96-well plate, cells were washed and 100 µL of 10 µM of dichloro-dihydrofluorescein diacetate (DCFH-DA) was added to each well and incubated for 45 min in a humidified atmosphere at 37 °C. Fluorescence was measured at excitation and emission wavelengths of 485 and 520 nm, respectively (33).

Western blotting

Cells were seeded in 6-well plate overnight at a density of 3×10^5 cells per well. Following 24 h treatment with mesocarp crude extract/fractions or punicalagin, cells were washed twice with PBS and lysed by addition of lysis buffer (25 mM Tris pH 8.3, 10 mM potassium chloride, 1 mM ethylenediaminetetraacetic acid (EDTA) and 1% Triton X-100) containing protease inhibitor. The concentration of protein was determined using the Bicinchoninic assay. A total of 5 µg of total protein was subjected to Western blotting. Goat anti-CD36 (AF2519 (1:1000, 0.2 µg/mL) (R&D Systems)) and mouse β-actin (sc-47778 (1:10000, 20 ng/mL) (Santa Cruz Biotechnology Inc.)) were incubated overnight at 4 °C. Immunoreactive bands were detected by 1 h incubation with anti-goat (HAF017 (1:1000) (R&D Systems)) and anti-mouse (sc-2005 (1:10000) (Santa Cruz Biotechnology Inc.)) HRP-conjugated antibodies. Results were analyzed using Image Lab software (Bio-Rad Laboratories, Inc). The relative protein expression was normalized to β-actin.

Total phenolics assay

Total phenolic content was quantified using the Folin-Ciocalteu method (34). A total of 0.25 mL of extract was mixed with 3.5 mL of distilled water and 0.25 mL of Folin-Ciocalteu reagent. After 3 min, 1 mL of 20% sodium carbonate solution was added. The reaction mixture was incubated at 40 °C for 40 min, after which the absorbance was read at 685 nm against a blank. The total phenolic content was calculated with respect to gallic acid standard curve and results expressed in mg of gallic acid equivalent (GAE)/g lyophilized powder (LP).

Total flavonoids assay

The aluminum chloride (AlCl₃) method was used to estimate the total flavonoid content (35). A total of 150 µL of 5% aqueous sodium nitrite, 500 µL of extract and 2 mL of distilled water were incubated for 5 min. A total of 150 µL of 10% aqueous AlCl₃ was then added, and to which 1 mL of 1 M sodium hydroxide was added and the mixture was made up to 5 mL with distilled water. The absorbance was measured at 510 nm against a blank. Total flavonoid content was calculated with respect to quercetin standard curve and results expressed in mg of quercetin equivalent (QE)/g LP.

Hydrolyzable tannin assay

The method of Saad et al. (36) with slight modifications was adapted to quantify the hydrolyzable tannin content. The reaction mixture contained 5 mL of 2.5% (w/v) potassium iodate previously incubated at 30 °C for 7 min and 1 mL of extract. The absorbance was read at 550 nm after 2 min of incubation at 30 °C against blank. Hydrolyzable tannin was calculated with respect to tannic acid standard curve and results expressed in mg of tannic equivalent (TAE)/g LP.

High-resolution ultra-performance liquid chromatography-mass spectrometry (UPLC-ESI-QTOFMS) metabolites analysis.

The lyophilized pomegranate mesocarp extract/fractions were mixed with 5 mL methanol (MeOH) containing umbelliferone (10 µg/mL) as internal standard, using a Turrax mixer (11,000 rpm) for five 20 s periods, separating each period with 1 min intervals to prevent heating, then the extracts were vortexed vigorously and centrifuged at 3000 rpm for 30 min to remove debris and filtered using 22 µm pore size filter. An aliquot of 500 µL of each sample was placed on a (500 mg) C18 cartridge preconditioned with MeOH and H₂O. Samples were then eluted using 5 mL MeOH, the eluent was evaporated under a nitrogen stream, and the collected dry residue was resuspended in 500 µL MeOH. Three microliters of the supernatant were used for UPLC-MS analysis.

Chromatographic separation was completed on ACQUITY UPLC system (Waters, Milford, MA) equipped with an HSS T3 column (100 × 1.0 mm, particle size 1.8 µm; Waters) using the exact conditions cited in Characterization of compounds

was performed by the generation of the candidate formula with a mass accuracy limit of 10 ppm, and also considering RT (retention time), MS² data and reference literature (37,38).

Statistical analyses

Regression analysis was performed to calculate the dose response relationship of standard solutions used for calibration. Statistical analysis was achieved using the GraphPad Software (USA) (Prism, version 5.01). Significant differences were determined using one-way ANOVA ($P < 0.05$) followed by Tukey's tests or Dunnett's multiple comparison. Linear regression plots were generated and correlations were computed as Spearmen's correlation coefficient.

For mass spectrometry data processing for multivariate data analysis, an investigative analysis of the processed UPLC-MS data was achieved by principal component analysis (PCA) followed by applying supervised pattern recognition i.e. orthogonal partial least squares discriminate analysis (OPLS-DA) performed on the UPLCMS scaled data using SIMCA-P software (Version 14.0, Umetrics, Umeå, Sweden). OPLS-DA was employed to model the metabolite differences among the different extracts. The OPLS-DA model performance was assessed by monitoring R² and Q² values, where R² expresses the goodness of model fit, whereas Q² indicates the extent of model predictability. All variables were mean centered and scaled to Pareto variance according to the protocol characterized in Issa et al. (39).

Results

Antioxidant activity of pomegranate mesocarp crude extract and fractions

The antioxidant capacity of the pomegranate mesocarp fractions in terms of FRAP and ORAC values are shown in Figure 1. Punicalagin served as positive control being major in pomegranate mesocarp (19). The highest ORAC value

was detected in the ethyl acetate fraction (Figure 1a) while the *n*-butanol fraction showed the highest FRAP value (Figure 1b). Different concentrations of each sample were used to assess their ABTS^{•+}, DPPH[•] and O₂^{•-} scavenging and iron (II) chelating activity. The mesocarp crude extract and fractions as well as punicalagin showed dose dependent activities whereby the concentration at 50% antioxidant activity (AA₅₀) is shown in Table 1. Punicalagin demonstrated the highest radicals scavenging activity (Table 1). The *n*-butanol fraction was the most potent free radicals scavenger and iron (II) chelator followed by the ethyl acetate fraction. The aqueous residual fraction has generally comparable antioxidant activity to that of the crude extract, whereas DCM fraction was the least potent fraction. Pearson's correlations demonstrated that the antioxidant activities of the mesocarp fractions from the six monitored antioxidant assays was significantly ($P < 0.01$) correlated to their polyphenolic content (Table S1).

Anti-glycation activity of pomegranate mesocarp crude extract and fractions

To assess the anti-glycation activity of the mesocarp crude extract and fractions, 0.1 mg/mL or 1 mg/mL of each sample and punicalagin was incubated with BSA and the glycating agents glucose, ribose or MGO. Levels of fluorescent AGEs, Amadori products, protein carbonyl and AOPP were evaluated after 15 days.

At both concentrations tested, punicalagin, ethyl acetate, *n*-butanol and aqueous residual fractions, along with the crude extract, significantly counteracted ($P < 0.001$) the glucose-, ribose- and MGO-induced increase in fluorescent AGEs level (Figure 2). No alteration in the fluorescent AGEs level was observed in the presence of the DCM fraction. Punicalagin afforded highest protection by suppressing the formation of fluorescent AGEs at both concentrations tested. Among the mesocarp fractions, *n*-butanol fraction demonstrated highest inhibitory action, with a remarkable decrease

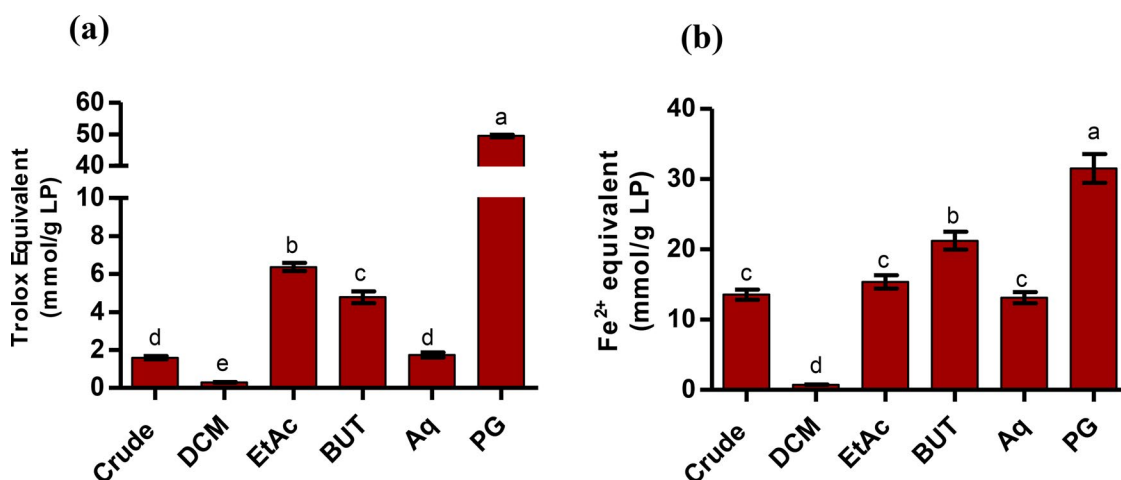


Figure 1. Antioxidant activity of the pomegranate mesocarp crude extract and fractions in terms of (a) ORAC and (b) FRAP values. DCM, dichloromethane fraction; EtAc, ethyl acetate fraction; BUT, *n*-butanol fraction; Aq, residual aqueous fraction; PG, punicalagin; LP, lyophilized powder. Bars represent mean \pm SEM mmol Fe²⁺/g LP of three independent assays performed in triplicate. Significance was assessed using one-way ANOVA followed by Tukey post Hoc; different letters between columns represent significant difference ($P < 0.05$) between samples.

Table 1. Antioxidant activity of the pomegranate mesocarp crude extract and fractions.

| Extract | IC ₅₀ values (µg/mL LP) | | | |
|---------|------------------------------------|------------------------------|---|-----------------------------|
| | ABTS ^{•+} scavenging | DPPH [•] scavenging | O ₂ ^{•-} scavenging | Fe ²⁺ chelation |
| Crude | 2.37 ± 0.07 ^c | 6.87 ± 0.55 ^{c,d} | 18.14 ± 1.05 ^{b,c} | 29.76 ± 1.62 ^c |
| DCM | 39.71 ± 2.45 ^d | 190.27 ± 17.54 ^e | 229.76 ± 19.97 ^d | 127.39 ± 10.04 ^d |
| EtAc | 1.86 ± 0.14 ^{b,c} | 5.06 ± 0.24 ^{b,c} | 12.39 ± 0.80 ^a | 11.80 ± 1.98 ^b |
| BUT | 1.26 ± 0.08 ^{a,b} | 3.733 ± 0.30 ^{a,b} | 10.23 ± 1.22 ^a | 5.95 ± 0.61 ^a |
| Aq | 2.75 ± 0.13 ^c | 7.85 ± 0.83 ^d | 21.60 ± 0.89 ^c | 26.44 ± 1.62 ^c |
| PG | 1.03 ± 0.18 ^a | 3.02 ± 0.34 ^a | 12.88 ± 0.27 ^{a,b} | 21.40 ± 2.62 ^c |

DCM, dichloromethane fraction; EtAc, ethyl acetate fraction; BUT, *n*-butanol fraction; Aq, residual aqueous fraction; PG, punicalagin; LP, lyophilized powder. Data represent mean IC₅₀ ± SEM of three independent assays performed in triplicate. Significance was assessed using one-way ANOVA followed by Tukey post Hoc; different superscripts between rows in individual columns represent significant difference (P < 0.05) between extracts.

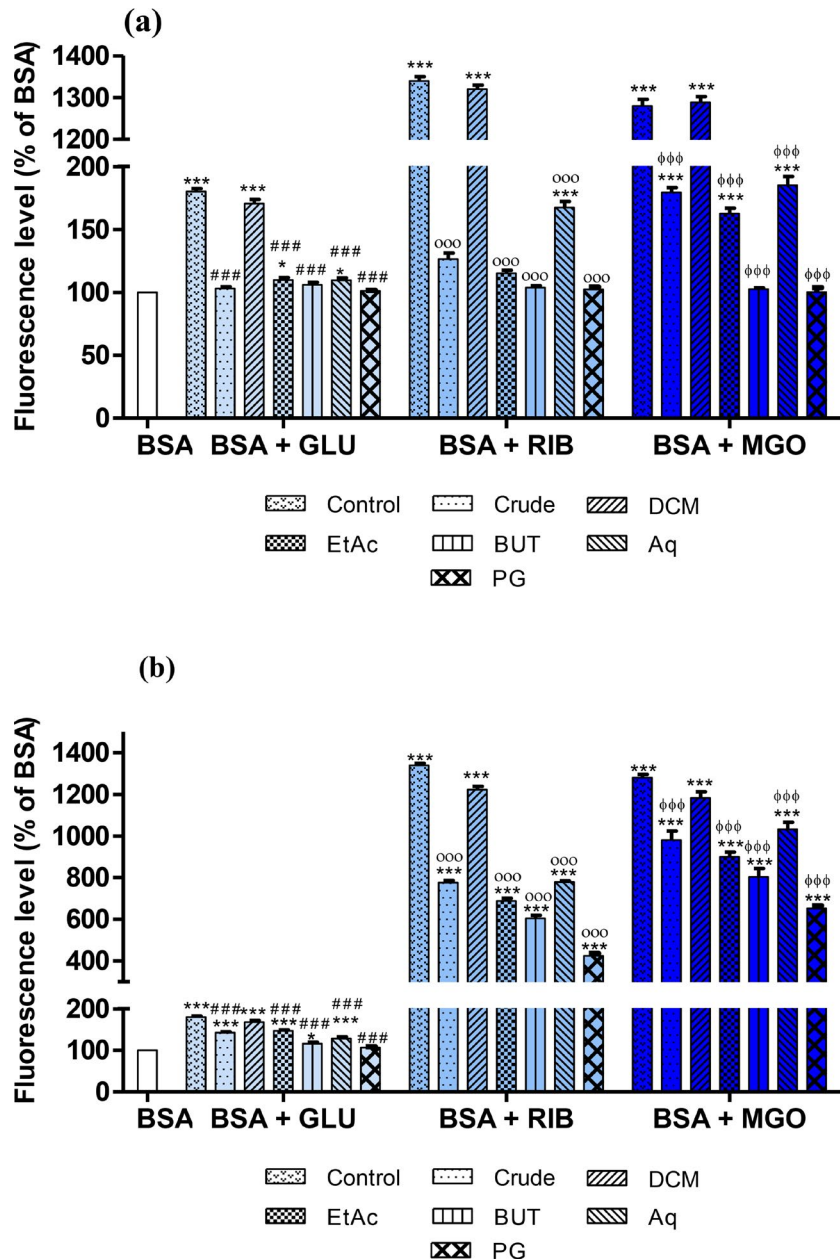


Figure 2. Effect of (a) 1 mg/mL and (b) 0.1 mg/mL of pomegranate mesocarp crude extract and fractions on formation of fluorescent AGEs in BSA exposed to glucose, ribose and methylglyoxal. GLU, glucose; RIB, ribose; MGO, methylglyoxal; DCM, dichloromethane fraction; EtAc, ethyl acetate fraction; BUT, *n*-butanol fraction; Aq, residual aqueous fraction; PG, punicalagin; LP, lyophilized powder. Data expressed as mean values ± SEM of three independent assays performed in duplicate. Significance was assessed using one-way ANOVA; *P < 0.05, ***P < 0.001 (vs. BSA); ###P < 0.001 (vs. BSA + GLU); ###P < 0.001 (vs. BSA + RIB); ###P < 0.001 (vs. BSA + MGO).

in fluorescent AGEs level in MGO-glycated BSA at 1 mg/mL (Figure 2a).

With the exception of the DCM fraction, the different mesocarp fractions and punicalagin dose dependently suppressed the formation of Amadori products in glucose-, ribose- and MGO-glycated BSA (Figure 3). At 1 mg/mL, level of Amadori products was significantly ($P < 0.001$) lower than their glycated counterparts. In addition, 0.1 mg/mL of punicalagin as well as the ethyl acetate and *n*-butanol fractions significantly suppressed the formation of Amadori products in BSA exposed to the three glycyating agents. At the same concentration, the crude extract and aqueous residual fraction did not show any significant activity against BSA glycosylation, while both samples significantly inhibited

BSA ribosylation as demonstrated by the reduced Amadori products

While glucose induced only a 9.6% increase in protein carbonyl level (Figure 4a(i)), ribose and MGO elevated the accumulation of protein carbonyl by 74.3% and 93.8%, respectively (Figure 4b(i) and c(i)). In glucose-glycated BSA, punicalagin at both concentrations in addition to the crude extract and ethyl acetate fraction at 1 mg/mL significantly ($P < 0.05$) suppressed accumulation of protein carbonyl. In the ribose- and MGO-glycated BSA, with the exception of the DCM fraction, all the fractions in addition to punicalagin significantly ($P < 0.001$) inhibited accumulation of protein carbonyl.

Glucose induced a 4.2 folds accumulation in AOPP level in BSA (Figure 4a(ii)). At both concentrations tested,

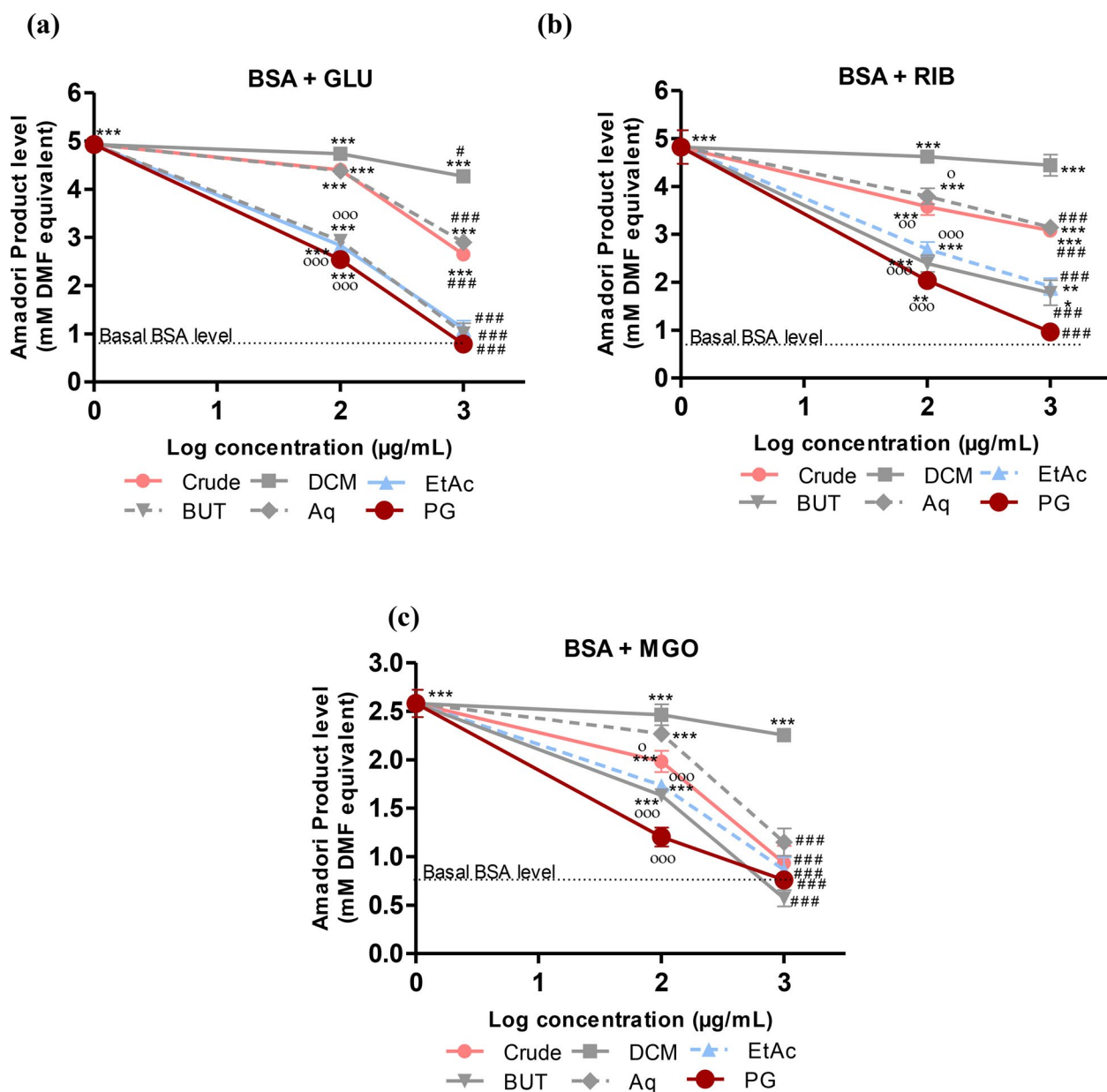


Figure 3. Effect of pomegranate mesocarp crude extract and fractions on fructosamine level in BSA exposed to (a) glucose, (b) ribose and (c) methylglyoxal. GLU, glucose; RIB, ribose; MGO, methylglyoxal; DCM, dichloromethane fraction; EtAc, ethyl acetate fraction; BUT, *n*-butanol fraction; Aq, residual aqueous fraction; PG, punicalagin; LP, lyophilized powder. Data expressed as mean values \pm SEM of three independent assays performed in duplicate. Significance was assessed using one-way ANOVA; * $P < 0.05$, ** $P < 0.01$, *** $P < 0.001$ (vs. BSA); * $P < 0.05$, *** $P < 0.001$ (vs. glycyating agent at 1 mg/mL); $^{\circ}P < 0.05$, $^{\circ\circ}P < 0.01$, $^{\circ\circ\circ}P < 0.001$ (vs. glycyating agent at 0.1 mg/mL).

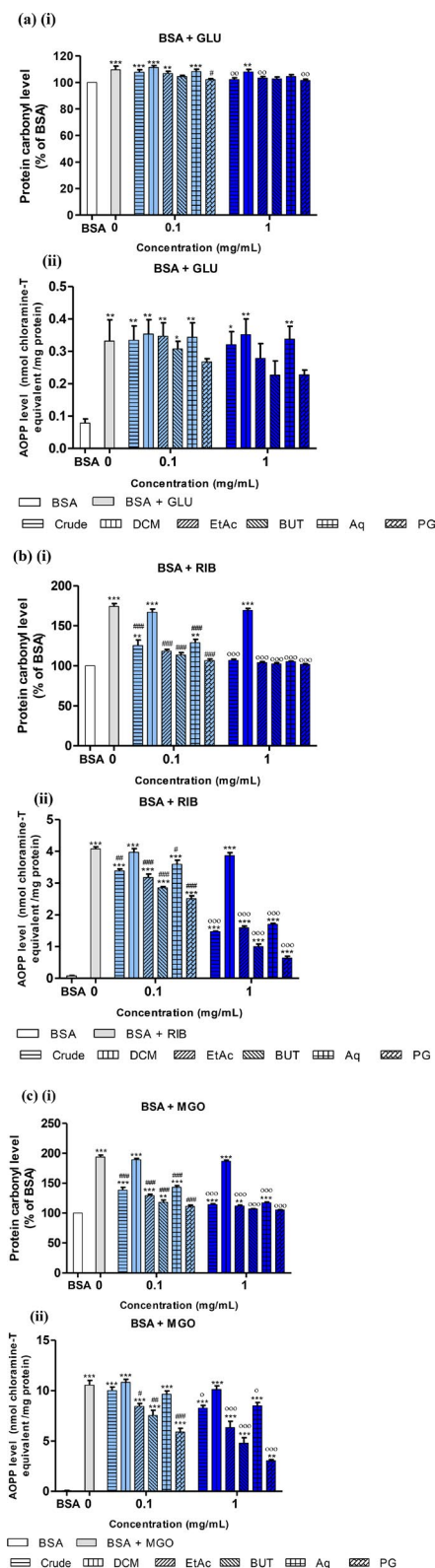


Figure 4. Effect of 1 mg/mL and 0.1 mg/mL of pomegranate mesocarp crude extract and fractions on (i) protein carbonyl and (ii) AOPP levels in BSA exposed (a) glucose, (b) ribose and (c) MGO. GLU, glucose; RIB, ribose; MGO, methylglyoxal; DCM, dichloromethane fraction; EtAc, ethyl acetate fraction; BUT, *n*-butanol fraction; Aq, residual aqueous fraction; PG, punicalagin; LP, lyophilized powder. Data expressed as mean values \pm SEM of three independent assays performed in duplicate. Significance was assessed using one-way ANOVA; * $P < 0.05$, ** $P < 0.01$, *** $P < 0.001$ (vs. BSA); # $P < 0.05$, ## $P < 0.01$, ### $P < 0.001$ (vs. glycosylating agent at 0.1 mg/mL); ° $P < 0.05$, °° $P < 0.01$, °°° $P < 0.001$ (vs. glycosylating agent at 1 mg/mL).

n-butanol fraction and punicalagin induced a non-significant decrease in the level of AOPP while only 1 mg/mL of ethyl acetate fraction demonstrated a non-significant decrease in AOPP level. In ribosylated BSA, the level of AOPP was 51.6 folds higher than that of unglycated BSA (Figure 4b(ii)). While the DCM fraction did not show any activity at both concentrations, the crude extract as well as the ethyl acetate, *n*-butanol and aqueous residual fractions significantly ($P < 0.05$) reduced the level of AOPP. In the case of MGO-glycated BSA, the level of AOPP was 133.5 folds higher than native BSA. With the exception of the DCM fraction, all the other fractions, the crude extract and punicalagin significantly ($P < 0.05$) inhibited AOPP level at 1 mg/mL.

Cellular protective effect pomegranate mesocarp crude extract and fractions and punicalagin

Following 24 h treatment with 10 μ g/mL of the fractions, no significant cell death was observed compared to control cells, as demonstrated by the MTT and LDH release assays (Figure 5a). Since the crude extract has the ability to down-regulate the basal ROS level production (18), the effect of the mesocarp fractions on the production of this pro-oxidant was investigated following 24 h of incubation. Interestingly, ethyl acetate and *n*-butanol fractions ($P < 0.01$) maintained the ability to reduce the basal ROS level (Figure 5b). When treated with 10 μ g/mL of the crude extracts and the fractions, the ethyl acetate, *n*-butanol and aqueous residual fractions down-regulated the expression of CD36 (Figure 5c). Relative to the control, the DCM fraction increased the expression of CD36 by at most 0.5 folds.

Cell viability assays demonstrated no cytotoxicity induced by punicalagin (Figure 6a). Interestingly, punicalagin significantly ($P < 0.05$) promoted the mitochondrial metabolic activity as demonstrated using the MTT assay (Figure 6a(i)). Treatment of cells with 10 μ g/mL of punicalagin significantly decreased ROS level ($P < 0.001$) and down-regulated the expression of CD36.

Polyphenolic content of pomegranate mesocarp crude extract and fractions

The polyphenolic content was determined in terms of total phenolics, total flavonoids and hydrolyzable tannins levels (Table 2). The total phenolic content of pomegranate mesocarp fractions ranged between 40.09 to 639.11 mg GAE/g LP, with the highest level observed in the *n*-butanol fraction. In contrast, DCM fraction had the lowest phenolic content. The *n*-butanol and ethyl acetate fractions of the mesocarp were the richest in flavonoids. Both fractions had higher phenolic and flavonoid contents compared to the crude extract. The *n*-butanol, ethyl acetate and aqueous residual fractions had comparable levels of hydrolyzable tannins to that of the crude extract. The lowest hydrolyzable tannins content among the fractions was observed in the DCM fraction, with a value of 115.33 mg TAE/g LP.

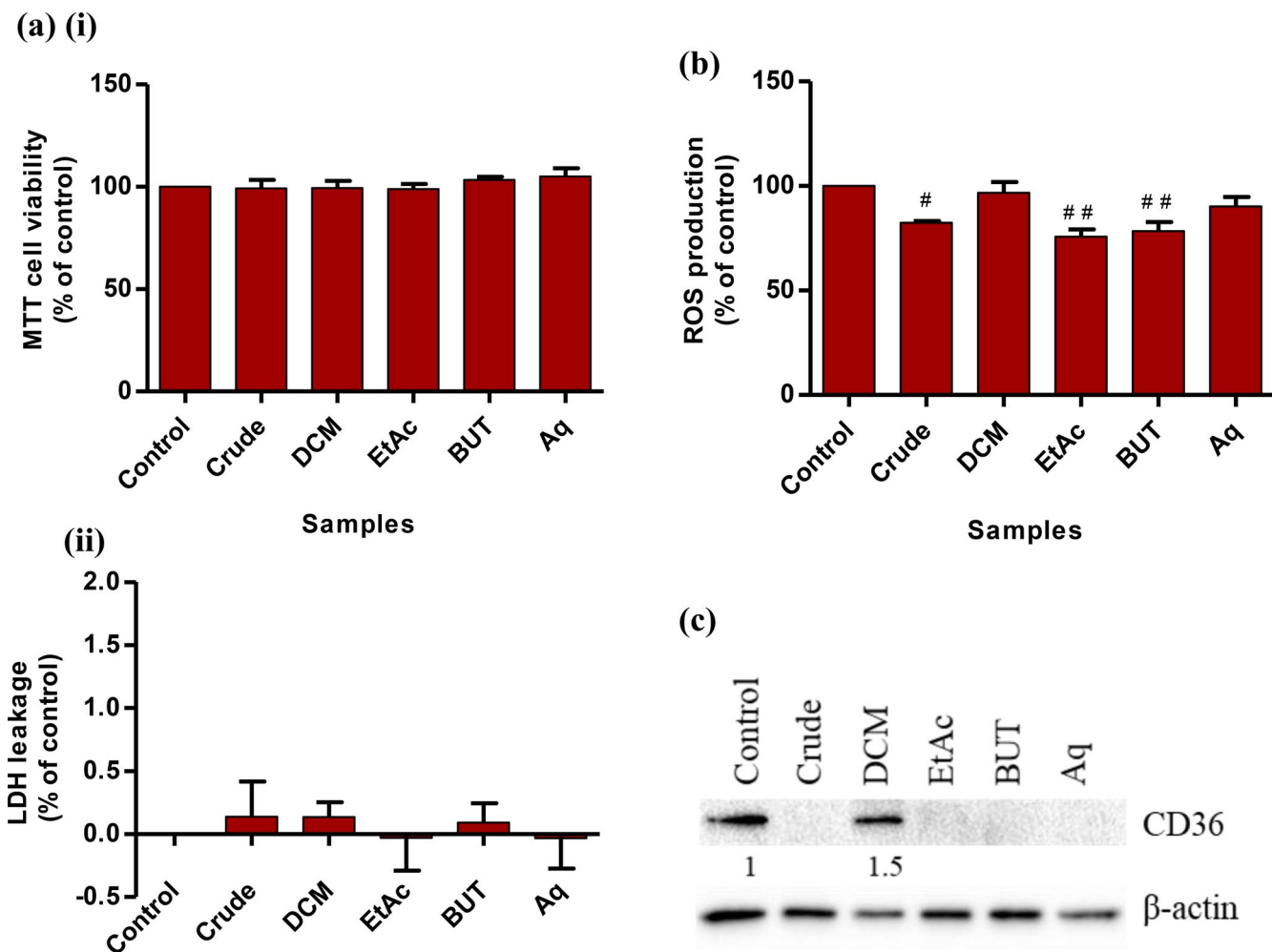


Figure 5. Effect of pomegranate mesocarp crude extract and fractions on (a) cell viability assessed by (i) MTT and (ii) LDH, (b) ROS production and (c) CD36 protein expression. DCM, dichloromethane fraction; EtAc, ethyl acetate fraction; BUT, *n*-butanol fraction; Aq, residual aqueous fraction. Data expressed as mean \pm SEM of three independent experiments performed in triplicate. Significance was assessed using one-way ANOVA followed by Dunnett's Multiple Comparison Test; [#] $P < 0.05$, ^{##} $P < 0.01$ (vs. control). Densitometry values are expressed relative to control and normalized against β -actin. Blots are representative of three independent experiments.

Ultra-performance liquid chromatography-mass spectrometry (UPLC-MS) metabolite profiles of pomegranate mesocarp fractions and their markers as analyzed by multivariate data analyses

Identification of the metabolite composition in pomegranate mesocarp crude extract and fractions was accomplished using non-targeted UPLC coupled to high resolution qTOF-MS. Metabolite profiles derived from UPLC-MS total ion chromatograms of the five extract/fractions of pomegranate mesocarp are presented in Figure 7. Metabolite assignments were made by comparing retention times relative to external standard and high resolution molecular mass and tandem mass spectra (exact mass and fragmentation pattern in negative ion mode) compared to reference literature and phytochemical dictionary of natural products database (40).

The crude extract of pomegranate mesocarp revealed the presence of a total of 45 chromatographic peaks belonging to hydrolyzable tannin and organic acid classes (Table 3). Ellagic and gallic acids and their derivatives were the major

detected metabolites in addition to (iso)citric acid. Ellagic acid was identified from its $[M-H]^-$ m/z 301 and MS² fragments m/z 283, 245, 229, and 185 whereas gallic acid $[M-H]^-$ at m/z 169 yielded MS² ion fragment ions at m/z 125. Ellagic and gallic acids have formerly been reported from pomegranate pericarp and juice (19,20,41,42,49). (Iso)citric acid $[M-H]^-$ at m/z 191 with MS² fragments m/z 173 and 111 is reported in pomegranate juice (41,50). Punicalagin consisting of gallagic acid, ellagic acid and hexose sugar, was also detected in the crude extract. It was identified from its $[M-H]^-$ m/z at 1083. Punicalagin isomers yielded MS² fragments at m/z 781 (loss of ellagic acid), m/z 601 (loss of a gallagic acid moiety) and m/z , 301 (loss of Hexahydrodiphenoyl (HHDP)). Moreover, punicalagin occurs in two natural isomeric forms *viz.*, α and β anomers (42,51). This is consistent with our data that revealed the presence of these two isomers in peaks 11 and 15 in pomegranate methanol crude extract. The major metabolite class detected in pomegranate mesocarp fractions was that of hydrolyzable tannins (Figure 8) in addition to some phenolic as well as organic and fatty acids (Table 3 and 4). Metabolites were

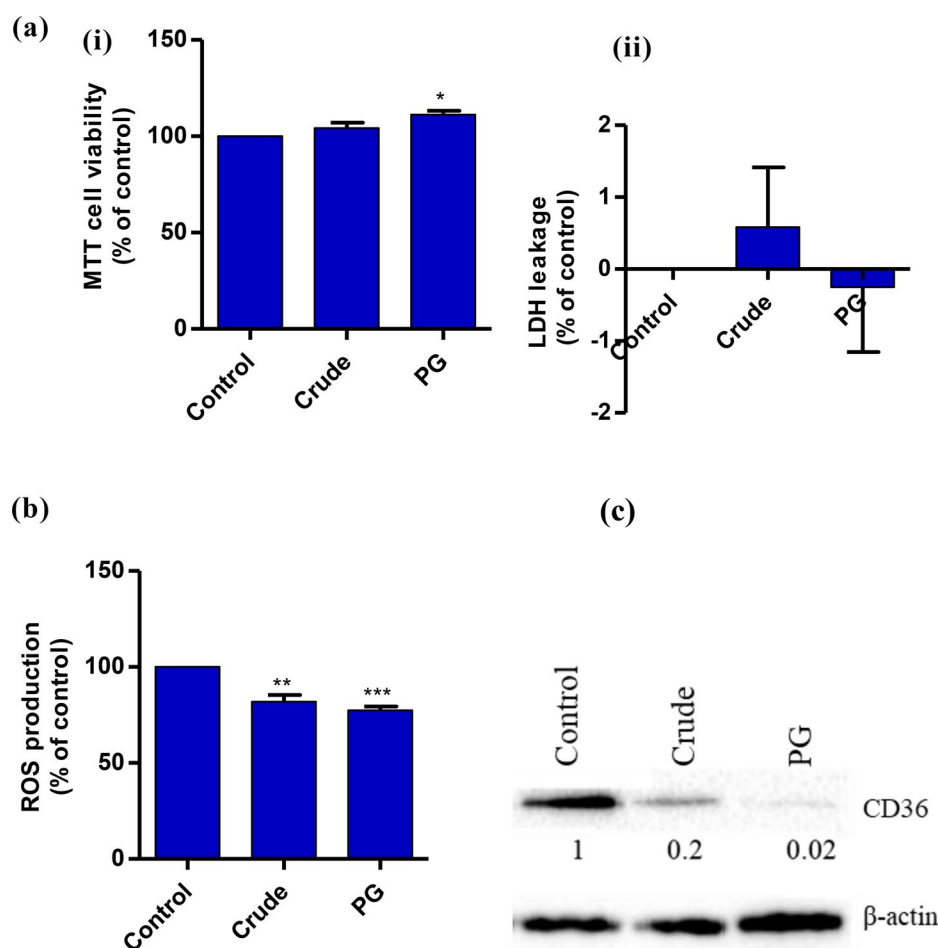


Figure 6. Effect of punicalagin on (a) cell viability assessed by (i) MTT and (ii) LDH, (b) ROS production and (c) CD36 protein expression. PG, punicalagin. Data expressed as mean \pm SEM of three independent experiments performed in triplicate. Significance was assessed using one-way ANOVA followed by Dunnett's Multiple Comparison Test; * $P < 0.05$, ** $P < 0.01$, *** $P < 0.001$ (vs. control). Densitometry values are expressed relative to control and normalized against β -actin. Blots are representative of three independent experiments.

Table 2. Polyphenolic content of the pomegranate mesocarp crude extract and fractions.

| Extract | TPC mg GAE/g LP | TFC mg QE/g LP | HTC mg TAE/g LP |
|---------|---------------------------------|---------------------------------|---------------------------------|
| Crude | 404.06 \pm 6.79 ^c | 365.15 \pm 5.67 ^b | 685.45 \pm 28.73 ^a |
| DCM | 40.09 \pm 1.66 ^d | 50.82 \pm 7.71 ^c | 115.32 \pm 6.15 ^b |
| EtAc | 557.46 \pm 3.66 ^b | 684.49 \pm 20.61 ^a | 773.81 \pm 32.63 ^a |
| BUT | 639.11 \pm 13.52 ^a | 754.72 \pm 25.30 ^a | 800.94 \pm 32.29 ^a |
| Aq | 415.84 \pm 9.36 ^c | 353.36 \pm 11.93 ^b | 690.39 \pm 29.50 ^a |

DCM, dichloromethane fraction; EtAc, ethyl acetate fraction; BUT, *n*-butanol fraction; Aq, residual aqueous fraction; TPC, total phenolic content; TFC, total flavonoid content; HTC, hydrolyzable tannin content; GAE, gallic acid equivalent; QE, quercetin equivalent; TAE, tannic acid equivalent; LP, lyophilized powder. Data represent mean \pm SEM of three independent assays performed in triplicate. Significance was assessed using one-way ANOVA followed by Tukey post Hoc; different letters between rows in individual columns represent significant difference ($P < 0.05$) between extracts.

eluted in descending polarity order, where phenolics were eluted first followed by their glycosides and fatty acids were eluted at last.

To identify metabolite markers unique for each fraction, fraction UPLC-MS metabolite profiles were modeled using

multivariate data analysis as X variable against each other and in relation to its biological effect as Y variable i.e., antioxidant and anti-glycation effects. Multivariate data analysis is employed to facilitate drug discoveries from plant extracts to avert the dereplication or isolation effort of a

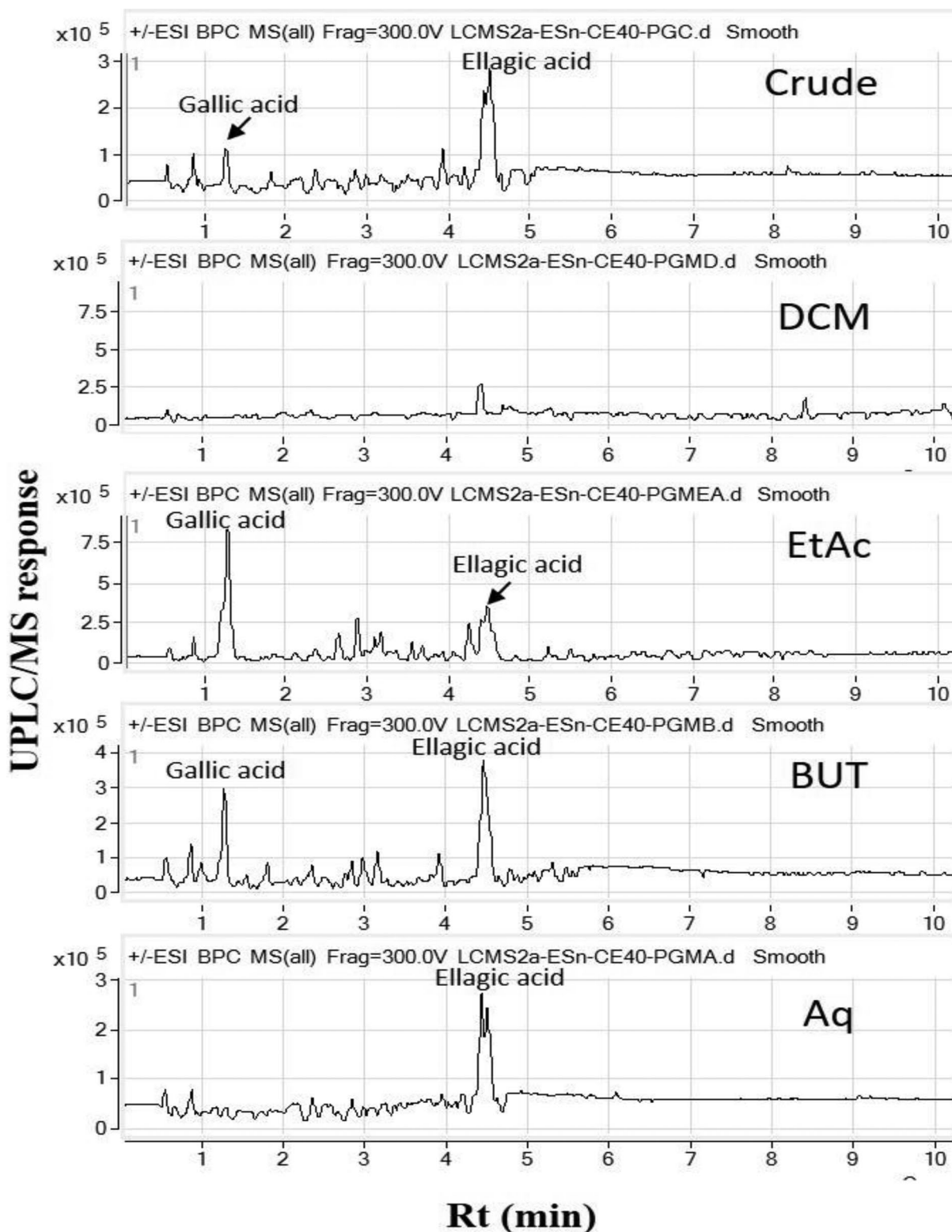


Figure 7. Representative UPLC-MS chromatogram of pomegranate mesocarp crude extract and fractions in negative ion mode. Rt: Retention time; DCM, dichloromethane fraction; EtAc, ethyl acetate fraction; BUT, *n*-butanol fraction; Aq, residual aqueous fraction.

known compound (54). Metabolite abundance dataset was modeled against the bioactivity data to detect metabolites that mediate antioxidant and anti-glycation effects. OPLS-DA modeling was established to explore the potential correlation between UPLC-MS derived metabolomes of the five tested samples (X variables) to their antioxidant and anti-glycation

potential (Y variables). The established OPLS-DA model (Figure 9) was validated for its performance to correlate the metabolite profiles of different specimens with their antioxidant and anti-glycation activities. These were demonstrated in the observed FRAP, Fe^{2+} chelating, $\text{ABTS}^{\bullet+}$ radical scavenging and DPPH^{\bullet} radical scavenging assays as well as

Table 3. Metabolites identified from UPLC-MS analysis of pomegranate mesocarp extract in negative ion mode.

| Peak | Assignment | RT | Precursor ion (m/z) | Error (ppm) | MS (m/z) | Molecular Formula | Product ions MS/MS | Class | Reference |
|------|---|-------|---------------------|-------------|-----------|---|---|--------------|------------|
| 1. | Malic acid | 0.674 | 133.0147 | -3.56 | 134.022 | C ₄ H ₆ O ₅ | 111, 104, 92, 71 | organic acid | (41) |
| 2. | (Isocitric acid I | 0.748 | 191.0205 | -6.28 | 192.0278 | C ₆ H ₈ O ₇ | 173, 111, 87, 129, 85, 57 | organic acid | (42,43) |
| 3. | HHDP hexoside | 0.779 | 481.0625 | -0.08 | 482.0697 | C ₃₀ H ₁₈ O ₁₄ | 301, 275, 257, 229, 203 | ellagitannin | (41,42) |
| 4. | (Isocitric acid II | 0.904 | 191.0197 | 0.14 | 192.027 | C ₆ H ₈ O ₇ | 173, 111, 87, 129, 85, 57 | organic acid | (42,43) |
| 5. | Galloyl hexose | 0.971 | 331.0671 | 0.06 | 332.0743 | C ₁₃ H ₁₆ O ₁₀ | 169, 125, 71, 59 | gallotannin | (41,42) |
| 6. | Galloyl hexose derivative | 0.977 | 421.0617 | 1.91 | 421.0617 | C ₁₅ H ₁₈ O ₁₄ | 331, 169, 125, 88, 59 | gallotannin | (19,41) |
| 7. | Gallic acid | 1.202 | 169.0141 | 0.77 | 170.0214 | C ₇ H ₆ O ₅ | 125, 97, 79, 69, 51 | organic acid | (19,41) |
| 8. | Galloyl-hex (Punicalin) | 1.358 | 781.0533 | -1.59 | 782.0615 | C ₃₄ H ₂₂ O ₂₂ | 721, 601, 575, 449, 301, 299, 273, 271, 245 | ellagitannin | (19,41) |
| 9. | Methyl (Isocitric acid I | 1.378 | 205.0357 | -1.26 | 206.0429 | C ₇ H ₁₀ O ₇ | 159, 124, 111, 87, 67 | organic acid | (19,41,42) |
| 10. | Galloyl-HHDP-hexose (Corilagin) | 1.54 | 633.073 | 0.77 | 634.0801 | C ₂₇ H ₂₂ O ₁₈ | 481, 301, 275, 249, 169, 125 | ellagitannin | (19,41,42) |
| 11. | HHDP-galloyl-hexose (Punicalagin) | 1.649 | 1083.0595 | 0.16 | 1084.0664 | C ₄₈ H ₂₈ O ₃₀ | 1083, 781, 601, 575, 463, 301 | ellagitannin | (19,41,42) |
| 12. | Bis-HHDP-hexose (Pedunculagin I) | 1.674 | 783.0682 | 0.84 | 784.0753 | C ₃₄ H ₂₄ O ₂₂ | 783, 481, 463, 301, 275, 249 | ellagitannin | (19,41,42) |
| 13. | Galloyl-HHDP-DHHDP-hex (granatin B) | 2.245 | 951.0751 | -0.03 | 952.0818 | C ₄₁ H ₂₈ O ₂₇ | 907, 783, 764, 745, 605, 481, 425, 301, 298, 98, 275 | ellagitannin | (19,42) |
| 14. | Bis-HHDP-hexose (Pedunculagin I) isomer | 2.265 | 783.0684 | 0.7 | 784.0754 | C ₃₄ H ₂₄ O ₂₂ | 783, 481, 463, 301, 275, 249 | ellagitannin | (19,41,42) |
| 15. | HHDP-galloyl-hexose (Punicalagin) | 2.534 | 1083.06 | -1.02 | 1084.068 | C ₄₈ H ₂₈ O ₃₀ | 1083, 781, 601, 575, 301, 275 | ellagitannin | (19,41,42) |
| 16. | Digalloyl-galloyl-hexose | 2.713 | 1085.0754 | -0.18 | 1086.0824 | C ₄₈ H ₃₀ O ₃₀ | 1085, 933, 783, 765, 633, 631, 601, 469, 451, 425, 301 | ellagitannin | (41) |
| 17. | Ellagic acid derivative/ Granatin A | 2.741 | 799.0633 | 0.41 | 800.0705 | C ₃₄ H ₂₄ O ₂₃ | 479, 301, 299, 275, 273 | ellagitannin | (19,44) |
| 18. | Galloyl-HHDP-hexoside (Corilagin) | 2.815 | 633.0739 | -1.1 | 634.0813 | C ₂₇ H ₂₂ O ₁₈ | 301, 275, 249, 169 | ellagitannin | (19,41,42) |
| 19. | Methyl gallate | 2.872 | 183.0299 | 0.16 | 184.0371 | C ₈ H ₈ O ₅ | 124, 78 | ellagitannin | (44) |
| 20. | Galloyl-bis-HHDP-hexoside (Casuarinin) | 2.931 | 935.0798 | 0.04 | 936.0868 | C ₄₁ H ₂₈ O ₂₆ | 917, 873, 783, 659, 633, 615, 571, 481, 419, 365, 329, 301, 299, 275, 249 | ellagitannin | (19,42) |
| 21. | Brevifolin carboxylate | 2.984 | 291.0149 | -0.66 | 292.0221 | C ₁₃ H ₆ O ₈ | 247, 219, 191, 173, 147, 145 | Ellagitannin | (19,42) |
| 22. | Brevifolin | 2.988 | 247.0249 | -0.03 | 248.0321 | C ₁₂ H ₈ O ₆ | 219, 191, 173, 147, 145 | ellagitannin | (44) |
| 23. | Digalloyl-HHDP-hex (Pedunculagin II) | 3.135 | 785.0849 | -0.35 | 786.0918 | C ₃₄ H ₂₆ O ₂₂ | 633, 615, 483, 419, 313, 301, 275, 249, 169 | ellagitannin | (19,42) |
| 24. | Unknown | 3.281 | 813.0792 | 0.52 | 814.0861 | C ₂₈ H ₂₀ O ₂₃ | 651, 479, 300, 99, 298, 98, 275 | ellagitannin | - |
| 25. | Galloyl-HHDP-hexoside (Corilagin) | 3.299 | 633.0735 | 0 | 634.0806 | C ₂₇ H ₂₂ O ₁₈ | 463, 301, 275, 249, 169 | ellagitannin | (19,41,42) |
| 26. | Unknown | 3.316 | 305.0698 | 9.9 | 306.0768 | C ₈ H ₁₀ O ₂ | 147, 96, 96, 79, 96, 59 | ellagitannin | - |
| 27. | Unknown | 3.372 | 323.041 | -0.51 | 324.0483 | C ₁₄ H ₁₂ O ₉ | 191, 175, 161, 147, 131, 119, 105 | ellagitannin | - |
| 28. | Ellagic acid-O-hexoside | 3.462 | 463.0522 | -0.58 | 464.0594 | C ₂₀ H ₁₆ O ₁₃ | 301, 257, 229 | ellagitannin | (19,41,42) |
| 29. | Digallic acid | 3.644 | 321.0249 | 0.87 | 322.0322 | C ₁₄ H ₁₀ O ₉ | 169, 125 | gallotannin | (45) |
| 30. | Digalloyl-HHDP-hexoside (Pedunculagin II) | 3.656 | 785.0836 | 0.09 | 786.0915 | C ₃₄ H ₂₆ O ₂₂ | 633, 615, 483, 419, 313, 300, 99, 275, 249, 169 | ellagitannin | (19,42) |
| 31. | Brevifolin | 3.835 | 247.0248 | 0.04 | 248.0321 | C ₁₂ H ₈ O ₆ | 219, 191, 173, 147, 145 | ellagitannin | (44) |
| 32. | Galloyl-HHDP-DHHDP-hexoside (Granatin B) | 3.883 | 951.0755 | -0.74 | 952.0825 | C ₄₁ H ₂₈ O ₂₇ | 933, 463, 301, 273, 245, 169 | ellagitannin | (19,42) |

(Continued)

Table 3. (Continued).

| Peak | Assignment | RT | Precursor ion (m/z) | Error (ppm) | MS (m/z) | Molecular Formula | Product ions MS/MS | Class | Reference |
|------|--|-------|---------------------|-------------|----------|---|--|--------------|------------|
| 33. | Phyllanembinin A (1-O-galloyl-2,4-tetrahydroxy dibenzofurandicarboxyl- hexose) | 3.984 | 615.0625 | 0.99 | 616.0694 | C ₂₇ H ₃₀ O ₁₇ | 463, 301, 169 | ellagitannin | (46) |
| 34. | Methyl brevifolin carboxylate | 4.047 | 305.0307 | -1.32 | 306.038 | C ₁₄ H ₁₀ O ₈ | 273, 245, 229, 217, 173, 145 | ellagitannin | (44) |
| 35. | Pelargonin A | 4.126 | 925.0952 | 0 | 926.1025 | C ₄₀ H ₃₆ O ₂₆ | 615, 301, 275, 273, 247 | ellagitannin | (47) |
| 36. | Digalloyl-HHDP-hexoside (Pedunculagin II) | 4.15 | 785.0837 | 0.37 | 786.0913 | C ₃₄ H ₃₆ O ₂₂ | 633, 615, 463, 419, 313, 301, 275, 249, 169 | ellagitannin | (19,42) |
| 37. | Tetragalloylhexose | 4.232 | 787.0996 | 0.88 | 788.1065 | C ₃₄ H ₃₈ O ₂₂ | 635, 617, 483, 465, 447, 421, 313, 295, 277, 235, 169, 125 | gallitannin | (42) |
| 38. | Ellagic acid-pentoside | 4.236 | 433.0407 | 1.5 | 434.0479 | C ₁₉ H ₁₄ O ₁₂ | 301, 300 | ellagitannin | (19,41) |
| 39. | Ellagic acid deoxyhexose | 4.278 | 447.0568 | 0.53 | 448.0639 | C ₂₀ H ₁₆ O ₁₂ | 301, 300 | Ellagitannin | (19,41,42) |
| 40. | Ellagic acid I | 4.556 | 300.9968 | 7.43 | 302.004 | C ₁₄ H ₆ O ₈ | 301, 283, 245, 229, 216, 200, 185, 173, 161, 145, 129, 117 | ellagitannin | (19,41,42) |
| 41. | Unknown | 4.624 | 965.089 | 1.22 | 966.0963 | C ₄₂ H ₃₀ O ₂₇ | 965, 933, 805, 663, 615, 463, 301 | ellagitannin | (48) |
| 42. | Ellagic acid II | 4.818 | 300.9989 | 0.31 | 302.0062 | C ₁₄ H ₆ O ₈ | 301, 283, 245, 229, 216, 200, 185, 173, 161, 145, 129, 117 | Ellagitannin | (19,41,42) |
| 43. | Ellagic acid III | 4.953 | 300.9986 | 1.3 | 302.0059 | C ₁₄ H ₆ O ₈ | 301, 283, 245, 229, 216, 200, 185, 173, 161, 145, 129, 117 | ellagitannin | (19,41,42) |
| 44. | Galic acid derivative | 4.977 | 507.1142 | 0.59 | 508.1214 | C ₂₃ H ₂₄ O ₁₃ | 313, 235, 220, 169, 125, 59 | gallotannin | - |
| 45. | 7-Hydroxycoumarin glucuronide | 5.029 | 337.0564 | 0.08 | 338.0638 | C ₁₅ H ₁₄ O ₉ | 307, 261, 231, 217, 201, 189, 176, 161, 145, 115 | gallotannin | - |

HHDP; Hexahydrodiphenol.

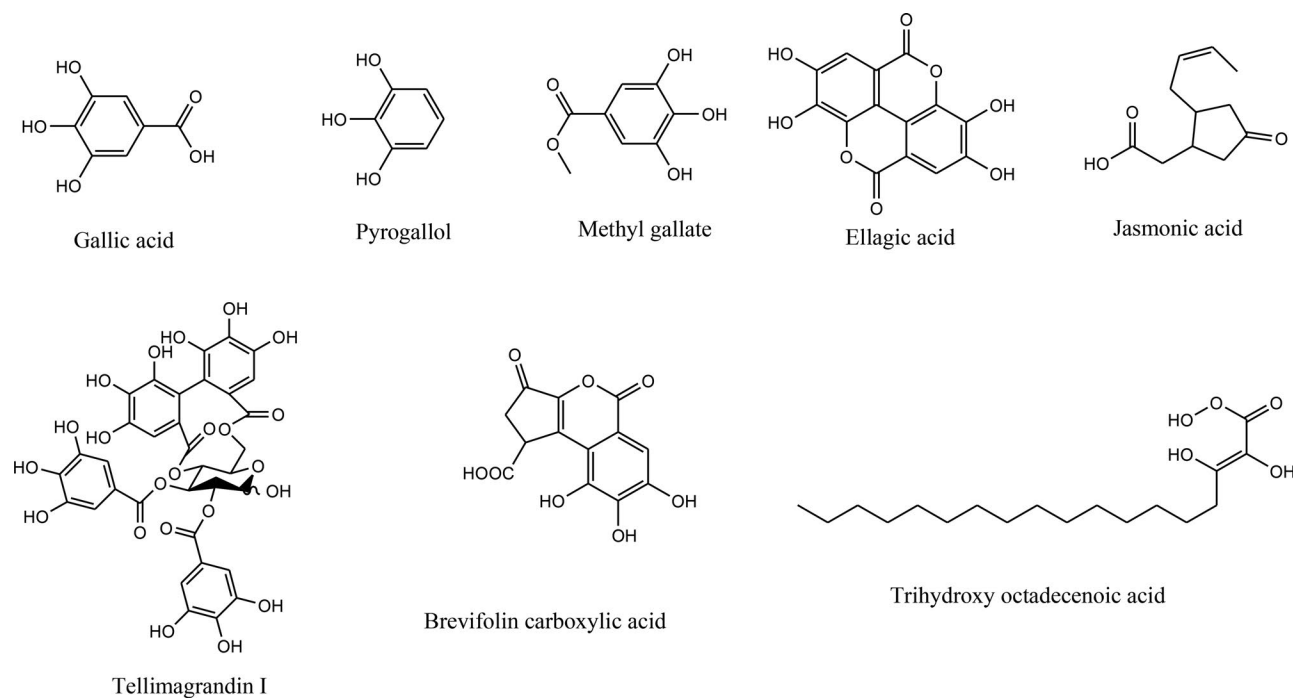


Figure 8. Chemical structures of discriminatory compounds identified in *P. granatum* mesocarp extract/fractions.

levels of fluorescent AGEs, Amadori products, protein carbonyl and AOPP for 20 iterations.

The ethyl acetate and *n*-butanol fractions were positioned on the left side of the plot (negative PC1 values), whereas on the right side, the pomegranate mesocarp crude extract, in addition to the DCM and aqueous fractions segregated (positive PC1 values) (Figure 9a). The validity of the UPLC-MS based OPLS model was assessed by calculating Q2 and R2 values of the models and were found greater than 0.4 and near 1. Commutation indicative analysis of 20 iterations presented reference distribution of R2/Q2 amounts and therefore exhibited statistical significance of these parameters, with the models showing a regression line crossing zero, with negative Q2 which denotes the model's justification (Supplementary Figures S1 and S2).

Discussion

Pomegranate mesocarp extract (PME) is known for its richness in polyphenols and is reported to exert high antioxidant capacity as well as anti-CD36 activity (18). PME was thus fractionated using DCM, ethyl acetate and *n*-butanol. The moderately polar solvents, ethyl acetate and *n*-butanol, were more effective in extracting phenolics, flavonoids and hydrolyzable tannins from the pomegranate mesocarp than the non-polar DCM. This is in line with findings of Šavikin et al. (55), whereby the non-polar fraction contained a lower phenolic content compared to the ethyl acetate, *n*-butanol as well as the aqueous fractions. This indicates the abundance of polar polyphenolic compounds in the pomegranate mesocarp, as previously reported (55). The ethyl acetate and *n*-butanol fractions of pomegranate mesocarp had higher levels of phenolics and flavonoids compared to the crude

extract due to the purification and concentrations of the polyphenolic compounds throughout the fractionation step (56).

The antioxidant propensity of the mesocarp fractions is attributed to their polyphenolic composition as demonstrated by their strong correlation. Polyphenols act as reducing agents to scavenge free radicals. In this process, the compounds get oxidized, which results in the generation of new radicals that are stabilized by the resonance of the aromatic nuclei due to electrons delocalization in the compounds (57,58). The H-donating hydroxyl group is also an essential structural characteristic that modulates the antioxidant potential of polyphenolic compounds (57). Thus, the higher the number of aromatic rings and hydroxyl groups in a compound, the greater is its antioxidant capacity (59). As such, the presence of compounds with several hydroxyl groups, such as gallic acid, pyrogallol, methyl gallate, brevifolin carboxylic acid in addition to complex compounds with at least 2 aromatic rings and several hydroxyl groups, such as tellimagrandin I, trigalloyl glucose, ellagic acid and tetra galloyl glucose in the ethyl acetate, *n*-butanol and/or aqueous residual fractions are accountable for the high antioxidant activities of these fractions. The polyphenols listed in Table 4 are the discriminatory metabolites that are responsible for differentiation and segregation of the different fractions. In addition to these compounds, punicalagin, galloyl hexoside, granatin B, pedunculagin I, galloyl-bis-HHDP-hexoside, casuarinin, brevifolin, corilagin and other unknown ellagitannins occur in almost equal amounts in the ethyl acetate, *n*-butanol and aqueous fractions.

The glycation capacity of the three glycyating agents, glucose, ribose and MGO, were evaluated by monitoring levels of fluorescent AGEs, Amadori products, protein carbonyl

Table 4. Discriminatory metabolites from OPLS model of mesocarp crude extract and fractions and their identification by UPLC-MS.

| Peak | Assignment | RT | Precursor ion (m/z) | Error (ppm) | MS (m/z) | Molecular Formula | MS ² ion fragments | Class | Crude | DCM | EtAc | BUT | Aq | Ref. |
|------|------------------------------|-------|---------------------|-------------|----------|---|--|--------------------------|-------|-----|------|-----|----|------------|
| 1. | Unknown | 0.734 | 96.9602 | — | — | — | 79.9, 78.9 | — | + | + | + | + | + | — |
| 2. | Galic acid | 1.192 | 169.0151 | -2.72 | 170.0225 | C ₇ H ₆ O ₅ | 125, 107, 97, 95, 79, 67, 51 | phenolic acid | + | + | + | + | + | (19,41) |
| 3. | Pyrogallol | 1.213 | 125.0243 | 1.09 | 126.0316 | C ₆ H ₆ O ₃ | 95, 79, 67, 51 | tannin | + | + | + | + | + | — |
| 4. | Methyl gallate | 2.868 | 183.0299 | 0.16 | 184.0371 | C ₈ H ₈ O ₅ | 125, 124, 78, 65 | phenolic acid derivative | + | + | + | + | + | (44) |
| 5. | Brevifolin carboxylic acid | 2.984 | 291.0149 | -0.66 | 292.0221 | C ₁₃ H ₈ O ₈ | 247, 219, 191, 173, 163, 145, 135, 119 | ellagitannin | + | + | + | + | + | (44) |
| 6. | Tellimagrandin I | 3.117 | 785.0849 | -1.09 | 786.0918 | C ₃₄ H ₂₆ O ₂₂ | 301, 275, 249, 169 | ellagitannin | + | + | + | + | + | (44,52) |
| 7. | Trigalloyl glucose | 3.593 | 635.0898 | 0.44 | 636.0969 | C ₂₇ H ₂₄ O ₁₈ | 483, 465, 313, 271, 221, 211, 169 | ellagitannin | + | + | + | + | + | (44) |
| 8. | Ellagic acid-O-hexoside | 3.484 | 463.0522 | -0.58 | 464.0594 | C ₂₈ H ₁₆ O ₁₃ | 301 | ellagitannin | + | + | + | + | + | (19,41,42) |
| 9. | Tetra galloyl glucose | 4.232 | 787.099 | 1.61 | 788.106 | C ₃₄ H ₂₈ O ₂₂ | 617, 456, 447, 313, 169 | ellagitannin | + | + | + | + | + | (44) |
| 10. | Ellagic acid | 4.489 | 301.0013 | -7.76 | 302.0086 | C ₁₄ H ₆ O ₈ | 283, 245, 229, 201, 185 | ellagitannin | + | + | + | + | + | (19,41,42) |
| 11. | Jasmonic acid | 7.68 | 209.1189 | -2.62 | 210.1261 | C ₁₂ H ₁₈ O ₃ | 165, 121, 80, 59 (100%) | organic acid | + | + | + | + | + | (53) |
| 12. | Trihydroxy octadecenoic acid | 8.372 | 329.2332 | 0.65 | 330.2404 | C ₁₈ H ₃₄ O ₅ | 211, 183, 171, 139, 127, 99, 57 | fatty acid | + | + | + | + | + | (54) |

DCM, dichloromethane fraction; EtAc, ethyl acetate fraction; BUT, n-butanol fraction; Aq, residual aqueous fraction.

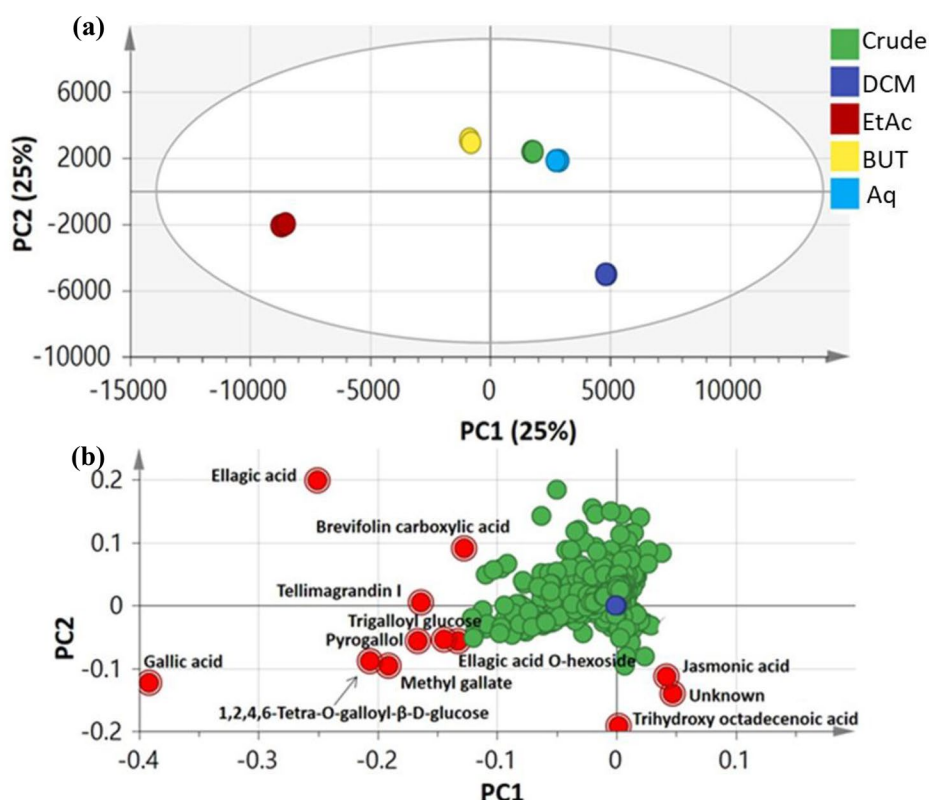


Figure 9. Orthogonal partial least squares discriminate analysis (OPLS-DA) of pomegranate mesocarp crude extract and its different fractions based on UPLC/MS data: (a) Score plot of PC1 vs. PC2 scores. (b) Loading plot for PC1 & PC2 contributing metabolites and their assignments. The metabolome clusters are located at the distinct positions in two-dimensional space described by two vectors of principal component 1 (PC1) = 25% and PC2=25%.

and AOPP levels. Ribose, being a more reactive unstable aldofuranose molecule, produced 7.4 folds higher level of fluorescent AGEs level than in the aldopyranose glucose-glucated BSA, making ribose more susceptible to react with amino groups of proteins (60). As compared to glucose, ribose also induced the accumulation of a higher level of protein carbonyl in BSA, indicating that the process of conversion of Amadori product to dicarbonyls in ribosylated BSA was faster than in glycosylated BSA. Being a dicarbonyl, MGO produces fewer intermediate products, as indicated by the level of Amadori products, to produce fluorescent AGEs (4). Different pomegranate mesocarp polyphenolic compounds, such as gallic acid, ellagic acid and punicalagin have been shown to exert anti-glycation activity (61,62). The free radical scavenging and metal chelating activities of the mesocarp fractions are the potential mechanisms through which they exert the anti-glycation activity as free radicals produced during the early stages of glycation participate in the glycation reaction (63). Polyphenols with at least 2 hydroxyl groups has been reported to exert anti-glycating activity by trapping MGO (64). As such, the presence of gallic acid, pyrogallol, methyl gallate, brevifolin carboxylic acid, tellimagrandin I, trigalloyl glucose, ellagic acid and tetra galloyl glucose in the ethyl acetate, *n*-butanol and/or aqueous residual fractions potentially account for the anti-glycation potency of these fractions. Moreover, the presence of vicinal hydroxyl group increases the activity of the polyphenolic compound (65). Polyphenolic compounds

also bind to proteins and thus prevent the interaction of the glycation agents due to the competitive binding of the polyphenolic compounds to the amino groups (66). The increase in AOPP level in BSA during the glycation process and the ability of polyphenolic compounds to suppress its formation have previously been shown (67). This indicates that other polyphenolic compounds present different samples potentially suppress AOPP formation by different mechanisms.

OPLS-DA score plot (Figure 9A) and loading plot (Figure 9B) explained the discrimination of samples in terms of metabolites mediating for its segregation. Examination of the loadings plot suggested that MS signals of ellagic and gallic acids together with jasmonic and trihydroxy octadecenoic acids contributed the most in extract/fractions discrimination (Figure 9B). Ellagic and gallic acids were found to be enriched in the ethyl acetate fraction and *n*-butanol fraction (negative PC1 score values) whereas the DCM fraction was augmented in jasmonic and trihydroxy octadecenoic acids with positive score plot in OPLS loading plot (Figure 9B). Such results are expected as DCM employs non-polar solvent in extraction and to encompass oxylipids versus abundance of phenolics in the polar *n*-butanol fraction. The distant clustering of ethyl acetate and *n*-butanol fractions was mostly attributed to the abundance of ellagic and gallic acids in these fractions and suggests that within the examined samples of pomegranate mesocarp segregation in OPLS-DA is largely influenced by ellagic and gallic acid

monomers. Ellagic and gallic acids have been reported to exhibit *in vitro* antioxidant activity (20,49) and control carbohydrate metabolism and hepatic glucose homeostasis via different mechanisms (68). Such reports might rationalize the high antioxidant and anti-glycation activities of the ethyl acetate and *n*-butanol fractions favoring for extraction of polar phenolic compounds and inclusion of these fractions in nutraceuticals used for sugar metabolic disorders. The OPLS-DA modeling of UPLC-MS metabolite profiles from the five fractions suggested that gallic and ellagic acids are potential contributors to the antioxidant and anti-glycation effects of the pomegranate mesocarp.

At cellular level, the polar polyphenolic-rich mesocarp fractions demonstrated antioxidant and anti-CD36 activities. These fractions were rich in antioxidant molecules, thus indicating that the decrease in ROS level below the basal level is liable to the presence of the polyphenolic compounds such as gallic acid, pyrogallol, methyl gallate, brevifolin carboxylic acid, telimagrandin I, trigalloyl glucose, ellagic acid and tetra galloyl glucose (discriminatory metabolites responsible for differentiation and segregation) as well as punicalagin, galloyl hexoside, granatin B, pedunculagin I, galloyl-bis-HHDP-hexoside, casuarinin, brevifolin, corilagin and other unknown ellagitannins (occurring in similar quantity) in the ethyl acetate, *n*-butanol and aqueous fractions. Unlike gallic and ellagic acids which are present in a large variety of plants, punicalagin is found in very few plants, including pomegranate. Since punicalagin is present in the polyphenolic-rich fractions and these fractions demonstrated good antioxidant and anti-CD36 activities, it was of interest to determine whether punicalagin mediate these activities. Interestingly, punicalagin demonstrated higher ability to reduce ROS level, as a consequence of the presence of several aromatic ring containing many hydroxyl groups (57–59). Moreover, punicalagin maintained the ability to suppress the expression of CD36 suggestive that it contributes to the anti-CD36 activities exerted by the ethyl acetate, *n*-butanol and aqueous fractions. The high antioxidant, anti-glycation and anti-CD36 of punicalagin indicate this polyphenolic compound is a promising therapeutic for the management of T2DM.

Conclusion

Our collective data showed that the high antioxidant and anti-glycation activities of the pomegranate crude extract as well as the ethyl acetate, *n*-butanol and aqueous residual fractions are attributed to their richness in phenolics, flavonoids and hydrolyzable tannins. The loading plots suggested that ellagic acid and gallic acid contributed to discrimination of the extract/fractions. In this line, the ethyl acetate and *n*-butanol fractions, which were enriched in these two compounds, demonstrated highest antioxidant and anti-glycation activities. At cellular level, a nontoxic dose of the polyphenolic-rich extract/fractions reduced the basal ROS level as well as down-regulated the protein expression of the AGEs receptor, CD36. The presence of punicalagin, in equal amount, in the extract/fractions is liable for this suppression in CD36 expression. This work demonstrated

the protective effect of the non-edible part of the pomegranate fruit and the involvement of different compounds in potentially exerting several anti-diabetic activities.

ORCID

Mohamed A. Farag  <http://orcid.org/0000-0001-5139-18634>

Funding

Dr Farag acknowledges the financial support received from the Alexander von Humboldt Foundation, Germany. We thank the Mauritius Herbarium, under the Ministry of Agro-Industry & Food Security, Mauritius for plant identification. Piteesha Ramlagan received the National Research and Innovation Chair Program studentship from the Mauritius Research and Innovation Council.

Disclosure statement

There are no conflicts to declare.

References

- Hameed I, Masoodi SR, Mir SA, Nabi M, Ghazanfar K, Ganai BA. Type 2 diabetes mellitus: from a metabolic disorder to an inflammatory condition. *World J Diabetes*. 2015;6(4):598–612. doi:10.4239/wjcd.v6.i4.598.
- International Diabetes Federation. *IDF diabetes atlas*. Belgium: International Diabetes Federation. 2019.
- Cantley J, Ashcroft FM. Correction to: Q&A: insulin secretion and type 2 diabetes: why do β -cells fail? *BMC Biol*. 2019;17(1):32. doi:10.1186/s12915-019-0650-8.
- Ott C, Jacobs K, Haucke E, Navarrete SA, Grune T, Simm A. Role of advanced glycation end products in cellular signaling. *Redox Biol*. 2014;2:411–29. doi:10.1016/j.redox.2013.12.016.
- Sompong W, Meeprom A, Cheng H, Adisakwattana SA. A comparative study of ferulic acid on different monosaccharide-mediated protein glycation and oxidative damage in bovine serum albumin. *Molecules*. 2013;18(11):13886–903. doi:10.3390/molecules181113886.
- Schaffer SW, Jong CJ, Mozaffari M. Role of oxidative stress in diabetes-mediated vascular dysfunction: unifying hypothesis of diabetes revisited. *Vascul Pharmacol*. 2012;57(5–6):139–49. doi:10.1016/j.vph.2012.03.005.
- Oguntibeju OO. Type 2 diabetes mellitus, oxidative stress and inflammation: examining the links. *Int J Physiol Pathophysiol Pharmacol*. 2019;11(3):45–63.
- Kuniyasu A, Ohgami N, Hayashi S, Miyazaki A, Horiuchi S, Nakayama H. CD36-mediated endocytic uptake of advanced glycation end products (AGE) in mouse 3T3-L1 and human subcutaneous adipocytes. *FEBS Lett*. 2003;537(1–3):85–90. doi:10.1016/S0014-5793(03)00096-6.
- Ohgami N, Nagai R, Ikemoto M, Arai H, Kuniyasu A, Horiuchi S, Nakayama H. CD36, a member of class B scavenger receptor family, is a receptor for advanced glycation end products. *Ann N Y Acad Sci*. 2001; 947:350–5. doi:10.1111/j.1749-6632.2001.tb03961.x.
- Sun Y, Scavini M, Orlando RA, Murata GH, Servilla KS, Tzamaloukas AH, Schrader R, Bedrick EJ, Burge MR, Abumrad NA, Zager PG. Increased CD36 expression signals monocyte activation among patients with type 2 diabetes. *Diabetes Care*. 2010;33(9):2065–7. doi:10.2337/dc10-0460.
- Soro-Paavonen A, Watson AM, Li J, Paavonen K, Koitka A, Calkin AC, Barit D, Coughlan MT, Drew BG, Lancaster GI, et al. Receptor for advanced glycation end products (RAGE)

- deficiency attenuates the development of atherosclerosis in diabetes. *Diabetes*. 2008;57(9):2461–9. doi:10.2337/db07-1808.
12. Zhu W, Li W, Silverstein RL. Advanced glycation end products induce a prothrombotic phenotype in mice via interaction with platelet CD36. *Blood*. 2012;119(25):6136–44. doi:10.1182/blood-2011-10-387506.
 13. Susztak K, Ciccone E, Mccue P, Sharma K, Böttinger EP. Multiple metabolic hits converge on CD36 as novel mediator of tubular epithelial apoptosis in diabetic nephropathy. *PLoS Med*. 2005;2(2):e45. doi:10.1371/journal.pmed.0020045.
 14. Guimarães EL, Empsen C, Geerts A, Van Grunsven LA. Advanced glycation end products induce production of reactive oxygen species via the activation of NADPH oxidase in murine hepatic stellate cells. *J Hepatol*. 2010;52(3):389–97. doi:10.1016/j.jhep.2009.12.007.
 15. Geloën A, Helin L, Geeraert B, Malaud E, Holvoet P, Marguerie G. CD36 inhibitors reduce postprandial hypertriglyceridemia and protect against diabetic dyslipidemia and atherosclerosis. *PLoS One*. 2012;7(5):e37633. doi:10.1371/journal.pone.0037633.
 16. Glatz JF, Angin Y, Steinbusch LK, Schwenk RW, Luiken JJ. CD36 as a target to prevent cardiac lipotoxicity and insulin resistance. *Prostaglandins Leukot Essent Fatty Acids*. 2013;88(1):71–7. doi:10.1016/j.plefa.2012.04.009.
 17. de Oliveira Silva C, Delbosc S, Araújo C, Monnier L, Cristol J-P, Pares-Herbute N. Pares-Herbute N. Modulation of CD36 protein expression by AGEs and insulin in aortic VSMCs from diabetic and non-diabetic rats. *Nutr Metab Cardiovasc Dis*. 2008;18(1):23–30. doi:10.1016/j.numecd.2006.07.008.
 18. Ramlagan P, Rondeau P, Planesse C, Neergheen-Bhujun VS, Fawdar S, Bourdon E, Bahorun T. *Punica granatum* L. mesocarp suppresses advanced glycation end products (AGEs)- and H₂O₂-induced oxidative stress and pro-inflammatory biomarkers. *J Funct Foods*. 2017; 29:115–26. doi:10.1016/j.jff.2016.12.007.
 19. Fischer UA, Carle R, Kammerer DR. Identification and quantification of phenolic compounds from pomegranate (*Punica granatum* L.) peel, mesocarp, aril and differently produced juices by HPLC-DAD-ESI/MS(n). *Food Chem*. 2011;127(2):807–21. doi:10.1016/j.foodchem.2010.12.156.
 20. Gil MI, Tomás-Barberán FA, Hess-Pierce B, Holcroft DM, Kader AA. Antioxidant activity of pomegranate juice and its relationship with phenolic composition and processing. *J Agric Food Chem*. 2000;48(10):4581–9. doi:10.1021/jf000404a.
 21. Benzie IF, Strain JJ. The ferric reducing ability of plasma (FRAP) as a measure of “antioxidant power”: the FRAP assay. *Anal Biochem*. 1996;239(1):70–6. doi:10.1006/abio.1996.0292.
 22. Huang D, Ou B, Hampsch-Woodill M, Flanagan JA, Prior RL. High-throughput assay of oxygen radical absorbance capacity (ORAC) using a multichannel liquid handling system coupled with a microplate fluorescence reader in 96-well format. *J Agric Food Chem*. 2002;50(16):4437–44. doi:10.1021/jf0201529.
 23. Re R, Pellegrini N, Proteggente A, Pannala A, Yang M, Rice-Evans C. Antioxidant activity applying an improved ABTS radical cation decolorization assay. *Free Radic Biol Med*. 1999;26(9–10):1231–7. doi:10.1016/S0891-5849(98)00315-3.
 24. Duan X, Jiang Y, Su X, Zhang Z, Shi J. Antioxidant properties of anthocyanins extracted from litchi (*Litchi chinensis* Sonn.) fruit pericarp tissues in relation to their role in the pericarp browning. *Food Chem*. 2007;101(4):1365–71. doi:10.1016/j.foodchem.2005.06.057.
 25. Dorman HJD, Koşar M, Kahlos K, Holm Y, Hiltunen R. Antioxidant properties and composition of aqueous extracts from *Mentha* species, hybrids, varieties, and cultivars. *J Agric Food Chem*. 2003;51(16):4563–9. doi:10.1021/jf034108k.
 26. Kumar M, Chandel M, Kumar S, Kaur S. Studies on the antioxidant/genoprotective activity of extracts of *Koeleruteria paniculata* laxm. *Am J Biomed Sci*. 2011;1:177–89. doi:10.5099/aj120200132.
 27. Wang W, Yagiz Y, Buran TJ, Nunes CN, Gu L. Phytochemicals from berries and grapes inhibited the formation of advanced glycation end-products by scavenging reactive carbonyls. *Food Res Int*. 2011;44(9):2666–73. doi:10.1016/j.foodres.2011.05.022.
 28. Meepprom A, Sompong W, Chan CB, Adisakwattana S. Isoferulic acid, a new anti-glycation agent, inhibits fructose- and glucose-mediated protein glycation in vitro. *Molecules*. 2013;18(6):6439–51. doi:10.3390/molecules18066439.
 29. Johnson RN, Metcalf PA, Baker JR. Fructosamine: a new approach to the estimation of serum glycosylprotein. An index of diabetic control. *Clin Chim Acta*. 1983;127(1):87–95. doi:10.1016/0009-8981(83)90078-5.
 30. Boyer F, Rondeau P, Bourdon E. Hyperglycemia induces oxidative damage in SW872 cells. *Arch Med Biomed Res*. 2014;1:66–78.
 31. Witko-Sarsat V, Friedlander M, Capeillère-Blandin C, Nguyen-Khoa T, Nguyen AT, Zingraff J, Jungers P, Descamps-Latscha B. Advanced oxidation protein products as a novel marker of oxidative stress in uremia. *Kidney Int*. 1996;49(5):1304–13. doi:10.1038/ki.1996.186.
 32. Mosmann T. Rapid colorimetric assay for cellular growth and survival: application to proliferation and cytotoxicity assays. *J Immunol Methods*. 1983;65(1–2):55–63. doi:10.1016/0022-1759(83)90303-4.
 33. Marimoutou M, Le Sage F, Smadja J, Lefebvre d’Hellencourt C, Gonthier M-P, Robert-Da Silva C. Antioxidant polyphenol-rich extracts from the medicinal plants *Antirhea borbonica*, *Doratoxylon apetalum* and *Gouania mauritiana* protect 3T3-L1 preadipocytes against H₂O₂, TNF α and LPS inflammatory mediators by regulating the expression of superoxide dismutase and NF- κ B genes. *J Inflamm (Lond)*. 2015;12:10. doi:10.1186/s12950-015-0055-6.
 34. Singleton VL, Rossi JA. Colorimetry of total phenolics with phosphomolybdic-phosphotungstic acid reagents. *Am J Enol Vitic*. 1965;16:144–58.
 35. Zhishen J, Mengcheng T, Jianming W. The determination of flavonoid contents in mulberry and their scavenging effects on superoxide radicals. *Food Chem*. 1999;64(4):555–9. doi:10.1016/S0308-8146(98)00102-2.
 36. Saad H, Bouhtoury FC, Pizzi A, Rod K, Charrier B, Ayed N. Characterization of pomegranate peels tannin extractives. *Ind Crops Prod*. 2012; 40:239–46. doi:10.1016/j.indcrop.2012.02.038.
 37. Khaled SE, Hashem FA-M, Shabana MH, Hammam A-MM, Madboli ANA, Al-Mahdy DA, Farag MA. A biochemometric approach for the assessment of *Phyllanthus emblica* female fertility effects as determined via UPLC-ESI-qTOF-MS and GC-MS. *Food Funct*. 2019;10(8):4620–35. doi:10.1039/c9fo00767a.
 38. Serag A, Baky MH, Döll S, Farag MA. UHPLC-MS metabolome based classification of umbelliferous fruit taxa: a prospect for phyto-equivalency of its different accessions and in response to roasting. *RSC Adv*. 2020;10(1):76–85. doi:10.1039/C9RA07841J.
 39. Issa MY, Mohsen E, Younis IY, Nofal ES, Farag MA. Volatiles distribution in jasmine flowers taxa grown in Egypt and its commercial products as analyzed via solid-phase microextraction (SPME) coupled to chemometrics. *Ind Crops Prod*. 2020; 144:112002. doi:10.1016/j.indcrop.2019.112002.
 40. Sánchez-Rabeneda F, Jáuregui O, Casals I, Andrés-Lacueva C, Izquierdo-Pulido M, Lamuela-Raventós RM. Liquid chromatographic/electrospray ionization tandem mass spectrometric study of the phenolic composition of cocoa (*Theobroma cacao*). *J Mass Spectrom*. 2003;38(1):35–42. doi:10.1002/jms.395.
 41. Mena P, Calani L, Dall’Asta C, Galaverna G, García-Viguera C, Bruni R, Crozier A, Del Rio D. Rapid and comprehensive evaluation of (poly)phenolic compounds in pomegranate (*Punica granatum* L.) juice by UHPLC-MSn. *Molecules*. 2012;17(12):14821–40. doi:10.3390/molecules171214821.
 42. Ambigaipalan P, de Camargo AC, Shahidi F. Phenolic compounds of pomegranate byproducts (outer skin, mesocarp, divider membrane) and their antioxidant activities. *J Agric Food Chem*. 2016;64(34):6584–604. doi:10.1021/acs.jafc.6b02950.
 43. Al-Olayan EM, El-Khadragy MF, Metwally DM, Moneim AEA. Protective effects of pomegranate (*Punica granatum*) juice on testes against carbon tetrachloride intoxication in rats. *BMC Complement Altern Med*. 2014; 14:164 doi:10.1186/1472-6882-14-164.
 44. Wu S, Tian L. Diverse phytochemicals and bioactivities in the ancient fruit and modern functional food pomegranate (*Punica*

- granatum*). *Molecules*. 2017; 22:1606. doi:10.3390/molecules22101606.
45. Abu-Reidah IM, Ali-Shtayeh MS, Jamous RM, Arráez-Román D, Segura-Carretero A. HPLC-DAD-ESI-MS/MS screening of bioactive components from *Rhus coriaria* L. (Sumac) fruits. *Food Chem*. 2015; 166:179–91. doi:10.1016/j.foodchem.2014.06.011.
 46. Zhang YJ, Abe T, Tanaka T, Yang CR, Kouno I. Phyllanemblinins A-F, new ellagitannins from *Phyllanthus emblica*. *J Nat Prod*. 2001;64(12):1527–32. doi:10.1021/np010370g.
 47. Latté KP, Kolodziej H. Pelargoninins, new ellagitannins from *Pelargonium reniforme*. *Phytochemistry*. 2000;54(7):701–8. doi:10.1016/S0031-9422(00)00176-X.
 48. Hanhineva K, Rogachev I, Kokko H, Mintz-Oron S, Venger I, Kärenlampi S, Aharoni A. Non-targeted analysis of spatial metabolite composition in strawberry (*Fragaria xananassa*) flowers. *Phytochemistry*. 2008;69(13):2463–81. doi:10.1016/j.phytochem.2008.07.009.
 49. Seeram NP, Adams LS, Henning SM, Niu Y, Zhang Y, Nair MG, Heber D. (). *In vitro* antiproliferative, apoptotic and antioxidant activities of punicalagin, ellagic acid and a total pomegranate tannin extract are enhanced in combination with other polyphenols as found in pomegranate juice. *J Nutr Biochem*. 2005;16(6):360–7. doi:10.1016/j.jnutbio.2005.01.006.
 50. Hassanen EI, Tohamy AF, Issa MY, Ibrahim MA, Farroh KY, Hassan AM. Pomegranate juice diminishes the mitochondria-dependent cell death and NF- κ B signaling pathway induced by copper oxide nanoparticles on liver and kidneys of rats. *Int J Nanomed*. 2019; 14:8905–22. doi:10.2147/IJN.S229461.
 51. Barbieri M, Heard CM. Isolation of punicalagin from *Punica granatum* rind extract using mass-directed semi-preparative ESI-AP single quadrupole LC-MS. *J Pharm Biomed Anal*. 2019;166:90–4. doi:10.1016/j.jpba.2018.12.033.
 52. Rahimi HR, Arastoo M, Ostad SN. A comprehensive review of *Punica granatum* (Pomegranate) properties in toxicological, pharmacological, cellular and molecular biology researches. *Iran J Pharm Res*. 2012;11(2):385–400.
 53. Segarra G, Jáuregui O, Casanova E, Trillas I. Simultaneous quantitative LC-ESI-MS/MS analyses of salicylic acid and jasmonic acid in crude extracts of *Cucumis sativus* under biotic stress. *Phytochemistry*. 2006;67(4):395–401. doi:10.1016/j.phytochem.2005.11.017.
 54. Farag MA, Gad HA, Heiss AG, Wessjohann LA. Metabolomics driven analysis of six *Nigella* species seeds via UPLC-qTOF-MS and GC-MS coupled to chemometrics. *Food Chem*. 2014;151:333–42. doi:10.1016/j.foodchem.2013.11.032.
 55. Šavikin K, Živković J, Alimpić A, Zdunić G, Janković T, Duletić-Laušević S, Menković N. Activity guided fractionation of pomegranate extract and its antioxidant, antidiabetic and antineurodegenerative properties. *Ind Crops Prod*. 2018; 113:142–9. doi:10.1016/j.indcrop.2018.01.031.
 56. Sannigrahi S, Kanti Mazuder U, Kumar Pal D, Parida S, Jain S. Antioxidant potential of crude extract and different fractions of *Enhydra fluctuans* Lour. *Iran J Pharm Res*. 2010;9(1):75–82.
 57. Cuvelier ME, Richard H, Berset C. Comparison of the antioxidative activity of some acid-phenols: structure-activity relationship. *Biosci Biotechnol Biochem*. 1992;56(2):324–5. doi:10.1271/bbb.56.324.
 58. Patel A, Patel A, Patel A, Patel NM. Determination of polyphenols and free radical scavenging activity of *Tephrosia purpurea* linn leaves (Leguminosae). *Pharmacognosy Res*. 2010;2(3):152–8. doi:10.4103/0974-8490.65509.
 59. Balasundram N, Sundram K, Samman S. Phenolic compounds in plants and agri-industrial by-products: antioxidant activity, occurrence, and potential uses. *Food Chem*. 2006;99(1):191–203. doi:10.1016/j.foodchem.2005.07.042.
 60. Wei Y, Chen L, Chen J, Ge L, He RQ. Rapid glycation with D-ribose induces globular amyloid-like aggregations of BSA with high cytotoxicity to SH-SY5Y cells. *BMC Cell Biol*. 2009;10:10. doi:10.1186/1471-2121-10-10.
 61. Liu W, Ma H, Frost L, Yuan T, Dain JA, Seeram NP. Pomegranate phenolics inhibit formation of advanced glycation endproducts by scavenging reactive carbonyl species. *Food Funct*. 2014;5(11):2996–3004. doi:10.1039/c4fo00538d.
 62. Kumagai Y, Nakatani S, Onodera H, Nagatomo A, Nishida N, Matsuura Y, Kobata K, Wada M. Anti-glycation effects of pomegranate (*Punica granatum* L.) fruit extract and its components *in vivo* and *in vitro*. *J Agric Food Chem*. 2015;63(35):7760–4. doi:10.1021/acs.jafc.5b02766.
 63. Yeh W-J, Hsia S-M, Lee W-H, Wu C-H. Polyphenols with anti-glycation activity and mechanisms of action: a review of recent findings. *J Food Drug Anal*. 2017;25(1):84–92. doi:10.1016/j.jfda.2016.10.017.
 64. Lo CY, Hsiao WT, Chen XY. Efficiency of trapping methylglyoxal by phenols and phenolic acids. *J Food Sci*. 2011;76(3):H90–H96. doi:10.1111/j.1750-3841.2011.02067.x.
 65. Piwowar A, Knapik-Kordecka M, Szczecińska J, Warwas M. Plasma glycooxidation protein products in type 2 diabetic patients with nephropathy. *Diabetes Metab Res Rev*. 2008;24(7):549–53. doi:10.1002/dmrr.885.
 66. Bhattacharjee A, Datta A. Mechanism of antiglycating properties of syringic and chlorogenic acids in *in vitro* glycation system. *Food Res Int*. 2015;77:540–8. doi:10.1016/j.foodres.2015.08.025.
 67. Sadowska-Bartosch I, Galiniak S, Bartosz G. Kinetics of glycooxidation of bovine serum albumin by glucose, fructose and ribose and its prevention by food components. *Molecules*. 2014;19(11):18828–49. doi:10.3390/molecules191118828.
 68. Khangholi S, Majid FA, Berwary NJ, Ahmad F, Aziz RB. The mechanisms of inhibition of advanced glycation end products formation through polyphenols in hyperglycemic condition. *Planta Med*. 2016;82(1–2):32–45. doi:10.1055/s-0035-1558086.